Bacterial Receptors but Not Anti-Phage Defence Mechanisms Determine Host Range for a Pair of *Pseudomonas aeruginosa* Lytic Phages

Authors:

Dea M. Müller[1]*, Julie D. Pourtois[1], Minyoung Kevin Kim[1], Bobby Targ, Elizabeth B. Burgener[2]

Carlos Milla[3], Robert McBride[1], Jyot D. Antani[4], Paul E. Turner[4,5], Jonathan L. Koff[6] and Paul L. Bollyky[1]*

Affiliations:

[1] Division of Infectious Diseases and Geographic Medicine, Department of Medicine, Stanford University School of Medicine, Stanford, California, USA

[2] Division of Pediatric Pulmonology & Sleep Medicine, Department of Pediatrics, Children's Hospital of Los Angeles, Keck School of Medicine at University of Southern California, Los Angeles, California, USA

[3] Center for Excellence in Pulmonary Biology, Division of Pulmonary Medicine, Department of Pediatrics, Stanford University, Stanford, CA, USA

[4] Center for Phage Biology and Therapy; Department of Ecology and Evolutionary Biology; and Quantitative Biology Institute, Yale University, New Haven, Connecticut, USA

[5] Program in Microbiology, Yale University, New Haven, Connecticut, USA

[6] Department of Medicine, Yale University, New Haven, Connecticut, USA

[*]**Correspondence:** Dea M. Müller (deam@stanford.edu) and Paul L. Bollyky (pbollyky@stanford.edu).

Abstract

Lytic bacteriophages (phage), viral predators of bacteria, offer a promising solution for treating bacterial infections. However, the narrow host range of phages limits the broad utility of individual phages, making the determinants of phage host range a subject of great interest. Here, we perform a genome-wide association study (GWAS) to identify bacterial genes associated with resistance or susceptibility to two lytic phages, OMKO1 and LPS-5, recently used in a clinical trial for patients with cystic fibrosis (pwCF). We analyzed 80 *Pseudomonas aeruginosa* clinical isolates collected from pwCF. For OMKO1, genes crucial for infection were associated with biofilm formation, exopolysaccharide synthesis, metabolism, porins, and flagellum assembly. We validate a critical role for flagellum genes in transposon mutagenesis experiments and functional assays. For LPS-5, genes associated with DNA repair, metabolism, and lipopolysaccharide biosynthesis are crucial for infection. We confirme the critical role for LPS/O-antigen in susceptibility to LPS-5. Interestingly, the presence of bacterial genes encoding bacterial defence mechanisms is not predictive of phage susceptibility. Instead, the relative abundance of several known defence elements is associated with the number of temperate phages within bacterial genomes. Together, our findings highlight the central role of receptors in determining phage host range, providing valuable insights for the development of phage-based therapies against bacterial infections.

Introduction

The emergence of antimicrobial-resistant (AMR) pathogens has become a critical global health concern, requiring urgent efforts to develop innovative therapeutic strategies[1]. Among these resistant pathogens, the gram-negative bacterium *Pseudomonas aeruginosa (Pa)* is particularly problematic; *Pa* accounts for roughly 10% of all hospital-acquired infections[2], including chronic infections such as diabetic ulcers and lung infections in individuals with cystic fibrosis[3]. The morbidity and mortality rates associated with both acute and chronic *Pa* infections can be as high as 40% [4].

There has been considerable interest in exploring bacteriophages as potential agents in the fight against AMR bacteria to address the urgent need for novel therapeutic approaches[5]. Lytic bacteriophages (phages) are viral predators of bacteria that use the bacterial cell to replicate. Lytic phages adsorb and infect host bacteria via cell receptors, replicate using cellular machinery, and cause host cell lysis to release new phage particles[6,7], enabling the initiation of new infection cycles in nearby cells. In contrast, temperate phages can enter a lysogenic cycle, during which their DNA integrates into the host chromosome as prophages or exists as plasmids, persisting until conditions trigger their transition to the lytic cycle.

The ongoing co-evolutionary arms races between bacteria and phages may result in the development of bacterial resistance mechanisms[8], while phages may evolve counterstrategies in response[9]. The evolution of phage resistance in target bacteria can limit the scope and efficacy of phage therapy - the use of phages to treat bacterial infections. Interest in phage therapy started in the early 20th century and increased over the last 50 years, with over 30,000 scientific articles on phages published during the period between 1965 and 2010, indicating substantial interest and investment in the field[10]. This has resulted in some successful use of phage therapy, particularly in compassionate use cases[11–16]. Despite promising results reported in some human case reports and studies, therapeutic failure has been documented in other studies, including clinical trials[17,18]. While the reasons for these failures are multifactorial, the limited host range of most phages remains a fundamental challenge to successful phage infections of bacterial pathogens.

For a successful phage infection, the phage must first adsorb (bind) onto one or more specific receptors on the cell surface, such as proteins, protein complexes or sugar moieties on LPS or other membrane structures. This results in many phages exhibiting a narrow host range, usually a subset of strains (genotypes) within the target bacterial species[19]. While this specificity can contributes to the safety of phage therapy because of limited infection of non-target cells, it also creates significant challenges for the development and application of phage therapy at a larger scale. Much effort is also dedicated to engineerring phages and increaseing their host range, and to simplifying the pipeline from diagnosis to treatment[20].

Bacterial resistance mechanisms, including innate immunity (e.g., Restriction-Modification systems (RM) and toxin-antitoxins systems[21–23]) and adaptive immunity (e.g., CRISPR elements and CRISPR-associated (cas) genes[24,25]), protect against phage predation. It has been shown that 30% of known Pa strains possess a type I-F CRISPR-Cas system, 6% a type I-E system and only very few also carry the type I-C CRISPR type [21]. However, the extent to which these defence systems contribute to therapeutic failure is unclear, as many of the identified mechanisms (e.g., abortive infection (Abi) systems, RM systems, and CRISPR), are highly specific, often targeting only a limited range of phages.

Addressing the biological limitations of phage infection remains a fundamental research focus and an essential step towards therapeutic success. In this work, we have studied phage susceptibility patterns in a set of 80 clinical *Pa* isolates collected from patients with cystic fibrosis (pwCF) using a pair of *Pa* phages, OMKO1[26] and LPS-5 , recently included in a human clinical trial of phage therapy in pwCF (NCT04684641). We first performed a Genome-Wide Association Study (GWAS) analysis to identify bacterial genes associated with phage resistance or susceptibility. We then sought to validate the results using a transposon mutagenesis library screening and functional analyses. Finally, we evaluate the effect of the presence of phage resistance mechanisms in the bacterial genome on lysis and prophage presence.

Results

Flagella-associated genes are significantly associated with OMKO1 phage infection

A lytic plaque assay was conducted to determine which of the 80 clinical *Pa* strains were susceptible to specific phages (Figure 1a). Combining this phenotypic data with the whole-genome sequences of the clinical isolates, we performed a Genome-Wide Association Study (GWAS) to identify genes associated with either phage susceptibility or resistance.

We then performed a functional enrichment analysis using enrichKEGG to identify enriched pathways given the large number of genes associated with phage infection. We found that biofilm formation and flagellar assembly were both significantly enriched in genes relevant to phage susceptibility (Figure 1b). We then differentiated between genes from these pathways associated with phage susceptibility and those associated with phage resistance. Notably, genes *fliY* and *fliP* in the flagellar assembly group are highlighted as important for OMKO1 phage susceptibility, while porin genes OprC and OprF are associated with phage resistance and susceptibility respectively (Figure 1c). The flagellum variants were mostly located on the intracellular portion of the flagellum (Figure 1d). Of the 80 clinical *Pa* isolates, only 4 were susceptible to OMKO1 as shown by the high susceptibility score from the lytic plaque assay (Figure 1e). This is consistent with the well-described loss of functional flagella associated with *Pa* colonization in pwCF[28]. With a swimming assay (Figure 1f), we show that flagella functionality explains the susceptibility pattern of OMKO1 of the lytic plaque assay (p-value = 0.01, Adjusted $R^2 = 0.6553$, Supplementary Figure 1), suggesting that OMKO1 uses the flagellum as its receptor.

To validate the crucial role for flagellum in OMKO1 infection, we conducted a transposon mutagenesis (Tn) assay (Figure 2a). Out of 49 identified genes that were significantly associated with OMKO1 phage susceptibility at a Multiplicity of Infection (MOI) of 0.1 (Fisher's test, p-value < 0.05), 28 genes were involved in flagellum structure and function (Figure 2b, Supplementary Figure 2). We then used the enrichKEGG package to explore which functional pathways were significantly enriched. We found that significant functional categories are linked to flagella assembly (enrichKEGG, p-value < 0.05) (Figure 2c). For a more detailed examination, we conducted a functional enrichment analysis using PANTHER (Figure 2d) which further identified that the particular flagella-associated pathways linked to OMKO1 phage infection include flagellum-dependent cell motility and flagellum organisation (PANTHER, p-value < 0.05). OMKO1 infection was associated with many flagella genes encoding proteins across the physical flagellum structure, from cytoplasmic to extracellular components (Figure 2e). Similar results were obtained at MOI 20 (Supplementary Figure 3).

We further validate the involvement of the functional flagellum as a receptor for phage OMKO1 by conducting a suppression assay assessing phage infection of OMKO1 for 7 clinical isolates (Figure 3a) and evaluate the functionality of the flagellum in these clinical isolates with a swimming assay (Figure 3b, c). We observed that the 5 bacterial strains resistant to the OMKO1 phage exhibited impaired flagella function, resulting in reduced swimming ability comparable to that of the *ΔfliC* strain. On the other hand, the 2 susceptible strains demonstrated functional flagella, as evidenced by their swimming area being comparable to the WT strain.

Many variants and mutations in flagella genes were identified to be associated with OMKO1 phage infection. The largest differences were observed in the genes *fliC*, *fliD*, *flgK*, and *flgL*. Sequence similarity for these genes was clustered according to percent identity within resistant and susceptible strains, and consensus sequences for both resistant and susceptible strains were generated (Supplementary Figure 4). The pairwise identity of the consensus sequences was assessed (*fliC*=52.7%, *fliD*=only resistant strains had a blast output, *flgK*=83.4%, *flgL*=72.6%). Additionally, single mutations were identified in other flagella genes, but no associations to phage infection could be identified with the current sample size (Table 1).

Table 1: Various bacterial sequences and mutations were identified to be associated with OMKO1 phage infection. The most significant differences were observed in the genes *fliC*, *fliD*, *flgK*, and *flgL*. Sequence similarity for these genes within resistant and susceptible strains was clustered, and

consensus sequences for both resistant and susceptible strains were generated. (Supplementary Figure 4). Single mutations were identified in other flagella genes.

Strains	Susceptibility	Swimming area [mm2]	Gene	Position (amino acid sequence)	Mutation (reference → strain)
CPA011	Resistant	8.1087	*flgE*	397	S->A
			fliH	56	P->A
			flgH	21	N->S
			fliR	60	S->P
			fliE	34	V->A
			fliY	67	A->E
			fliY	125	E->D
			fliY	130	K->R
CPA049	Resistant	10.30024	*fliH*	259	L->F
			fliH	10	N->S
			fliR	165	S->N
			fliR	60	S->P
CPA086	Resistant	44.48828	*fliE*	34	V->A
			fliR	60	S->P
CPA162	Resistant	10.30024	*flgB*	63	T->I
			flhA	26	V->I
			fliE	34	V->A
			fliR	60	S->P
			fliE	28	V->A
			fliF	21	K->Q
CPA434	Resistant	110.892	*fliE*	34	V->A
			flgF	92	A->T
CPA057	Susceptible	248.0824	*flhA*	26	V->I
			flgE	397	S->A
			flhB	49	I->M
			fliR	60	S->P
CPA351	Susceptible	136.7521	*fliE*	34	V->A
			fliR	60	S->P
			fliO	7	A->V

LPS-associated genes are associated with LPS-5 phage infection

Given the numerous genes identified by the GWAS in association with LPS-5 phage infection, a functional enrichment analysis was conducted to identify enriched pathways. We found several metabolic pathways and mismatch repair pathways that were significantly enriched and relevant to phage infection (Figure 4a). We then differentiated between genes from these pathways associated with phage susceptibility and those associated with phage resistance (Figure 4b).

In the Tn assay using MOI 0.1, 29 genes were found to be significantly associated with LPS-5 infection (Fisher's test, p-value < 0.05), including four genes related to lipopolysaccharide (LPS) biosynthesis (Figure 5a, Supplementary Figure 5). Enrichment analysis using the enrichKEGG identified DNA mismatch repair as the only significant pathway associated with LPS-5 infection (Figure 5b, p-value < 0.05). Further analysis using PANTHER revealed categories related with LPS function for the phage LPS-5 (Figure 5c). Some encode proteins involved in LPS biosynthesis pathways (Figure 5d). Similar results were obtained at MOI 20 (Supplementary Figure 6).

To validate the role of LPS as a receptor in LPS-5 infection, we conducted a suppression assay across various clinical isolates (Figure 6a). The function of the O-antigen in these clinical isolates was also assessed using a rugae O-AG/LPS assay. All five bacterial strains resistant to the LPS-5 phage did not form a colony biofilm rugae (rough colony morphotype), suggesting mutations in their O-antigen within the LPS (Figure 6b). Conversely, 2 out of the 5 susceptible strains exhibited a rugae phenotype, indicative of LPS containing the intact O-antigen.

Mutations in LPS biosynthetic genes in these strains were studied alongside with LPS-5 phage infection. The genes *migA* and *wzy* had the most mutations, with some mutations also found in the genes *ssg* and *wapH*. However, due to the limited sample size, no associations between single mutations and susceptibility to phage infection could be identified (Table 2).

Table 2: Mutations in LPS biosynthetic genes in these strains were identified to be associated with LPS-5 phage infection. Most mutations were observed in the genes *migA* and *wzy*, with some mutations also found in the genes *ssg* and *wapH*.

Strains	Susceptibility	Rugae	Gene	Position (amino acid sequence)	Mutation (reference → strain)
CPA011	Resistant	no rugae	*migA*	92	R->Q
			wapH	312	V->I
			wzy	No hits in blast	
CPA049	Resistant	no growth	*migA*	92	R->Q
CPA086	Resistant	no rugae	*ssg*	47	K->N
			migA	92	R->Q
CPA162	Resistant	no growth	*migA*	92	R->Q
			wzy	No hits in blast	
CPA434	Resistant	no rugae	*migA*	92	R->Q
			wzy	25	T->I
			wapH	322	T->A
			wzy	155	V->A
			wzy	24	A->V
			wzy	262	V->I
			wzy	85	L->I
			wzy	376	V->I
			wzy	182	V->A
			wzy	326	Q->H
CPA057	Susceptible	rugae	*migA*	92	R->Q
			wapH	160	A->G
			wzy	No hits in blast	
CPA166	Susceptible	no rugae	*migA*	92	R->Q
			wzy	No hits in blast	
CPA201	Susceptible	rugae	*migA*	92	R->Q
			wzy	No hits in blast	
CPA351	Susceptible	no rugae	*migA*	12	G->D
			wapH	322	T->A
			wzy	No hits in blast	
CPA482	Susceptible	no rugae	*wapH*	322	T->A
			migA	92	R->Q
			wzy	No hits in blast	

The presence of bacterial defence systems is not associated with lytic phage susceptibility

Bacterial defence systems were not identified in the GWAS, suggesting that these defence systems may not be involved in initial stages of phage infection. To confirm the potential involvement of bacterial defence systems in phage infection, we first screened the bacterial genomes of 80 clinical isolates and identified a total of 123 defence systems (Figure 7b). We then assessed the individual relationship between each defense system and phage susceptibility using a Wilcoxon test. For example, RM type I system was tested as shown in Figure 7c. The results revealed that no defence system was significantly associated with the phenotype of phage susceptibility or resistance (Wilcoxon test, p-value > 0.05 for all) (Figure 7d).

To consider the combined effect of these defence mechanisms on phage susceptibility, we included the defence systems depicted in Figure 7d in a Generalized Linear Model (GLM). This analysis reaffirmed the findings of the Wilcoxon analysis, demonstrating that none of the systems are significantly associated with susceptibility to either LPS-5 or OMKO1 susceptibility (GLM, p-value > 0.05) (Figure 7e).

Together, our comprehensive analysis of bacterial defence systems in clinical isolates suggests that these systems do not play a significant role in determining susceptibility or resistance to lytic phages such as LPS-5 and OMKO1.

The presence of bacterial defence systems is associated with temperate phage infection

To investigate the potential association between bacterial defence systems and temperate phage infection, we screened the genomes of clinical isolates for the presence of temperate phages using VIBRANT and BLAST. We first assessed the individual relationship between each system and temperate phages using a Wilcoxon test. The results showed that the presence of 4 defence systems, namely PDC-S02, PDC-M61, Helicase-DUF2290 and cas type I-F1 was significantly associated with the number of temperate phages (Wilcoxon test, p-value < 0.05 for all). Interestingly, two of these defence systems (PDC-202 and Helicase-DUF2290) exhibited a positive correlation with the number of phages, while the other two systems (PDC-M61 and Cas type I-F1) showed a negative correlation.

Next, to consider the combined effect of these defence mechanisms on the number of prophages, we included the significant defence systems in a Generalized Linear Model. This analysis re-confirmed the findings of the Wilcoxon analysis, demonstrating that the aforementioned defence systems were significantly associated with the number of prophages (GLM, p-value < 0.05 for all, Figure 7f).

Together, these results suggest that certain bacterial defence systems, such as PDC-S02, PDC-M61, Helicase-DUF2290, and cas type I-F1, may play a role in the regulation of temperate phage infection in clinical isolates. The observed positive and negative correlations between specific defence systems and the number of prophages highlight the complex interactions between bacteria and temperate phages.

Discussion

In this work, we investigated the bacterial genes that influence the host range of two lytic phages, OMKO1 and LPS-5, in a large set of *Pa* clinical isolates collected from pwCF. Our results implicate bacterial structures known to serve as receptors for these and other phages in phage susceptibility, which is consistent with the observation that the emergence of bacterial resistance to phages is often associated with the loss of receptor structures[29–31]. We further find roles for genes involved in bacterial metabolism, biofilm formation, and other cellular functions in phage susceptibility.

Our results demonstrate that the phage OMKO1 can utilize the flagellum as a receptor for host infection, which has previously been shown for other phages[32–37]. We speculate that the phage binds to a specific region of the flagellum, serving as a receptor, and then uses the flagellar motion to approach the bacterial surface. The evolution of bacterial resistance against flagellotropic phages is known to involve mutations and the downregulation of flagella[37]. Previous studies have established the role of the porin OprM as a receptor for phage OMKO1[26,32,38]. In our transposon mutagenesis study, the absence of a transposon insertion in the gene *oprM* gene made it impossible to draw any definitive conclusions. We speculate that upon reaching the bacterial body, the phage might interact with the entry receptor OprM and subsequently infect the bacterium[32,39]. Indeed, a closely related phage PhiKZ is known to use both the flagella and the type IV pilus as receptors[40].

Regarding the phage LPS-5, our results suggest that it uses the lipopolysaccharide, specifically the O-antigen, as a receptor for infecting its host, similar to many other phages that bind the O-antigen as their receptor[41,42]. This hypothesis is supported by the identification of three genes linked to the biosynthesis machinery of the O-antigen in the transposon mutagenesis assay. Our O-antigen experiments validate the hypothesis that the O-antigen serves as the receptor for phage LPS-5[43]. Other genes controlling rugae formation, such as those involved in quorum sensing, may also play a role in influencing rugae formation[44]. Further work will be necessary to confirm the role of the O-antigen as the receptor for LPS-5.

In addition to receptor structures, we found roles for genes involved in bacterial metabolism, biofilm formation, and other cellular functions in phage susceptibility. Experiments for both phages showed enrichment of numerous metabolic pathways in the GWAS and Tn assay, including fatty acid metabolism, amino acid metabolism, pyrimidine biosynthetic and pyrimidine metabolic processes, amino sugar and nucleotide sugar metabolism, glycolysis, citrate cycle and others. These findings are consistent with previous studies that have highlighted the relationship between phage infection and metabolic changes in host bacteria[45–47]. In one study, multi-phage resistance was found to be associated with reduced fitness in a PAO1 population, but not in clinical isolates. The authors hypothesized that

clinical strains, having co-evolved with phages, controlled phage infection not solely through direct modification of genes responsible for surface receptor biosynthesis, but rather through global regulation of cell metabolism[45]. Another study has shown that different *Pa* phages can not only deplete metabolites but also completely reorganize the metabolism in a phage- and infection-specific manner, eliciting an increase in pyrimidine and nucleotide sugar metabolism[46]. Thus, phage infection can exert considerable stress on bacteria, leading to alterations in their metabolic profiles.

Pathways for mismatch repair, particularly involving the protein MutL, and nucleotide excision repair were found to be linked with phage infection. Some viruses employ non-homologous end joining (NHEJ) for viral genome circularization, and the loss of NHEJ could potentially serve as an anti-viral strategy for the host bacteria[48]. Another study also identified mutations in genes unrelated to the corresponding phage receptor molecules but rather involving deletions in the DNA mismatch repair protein MutL[47].

Pathways associated with biofilm formation and exopolysaccharide biosynthesis were found to be linked with phage infection. This finding is consistent with a previous study that demonstrated changes in pathways associated with biofilm and exopolysaccharide production in phage-resistant *Pa* strains[47].

Surprisingly, the data presented here did not link the known phage defence systems present in these clinical isolates to susceptibility or resistance to the pair of phages studied. This finding contrasts with previous studies implicating defence mechanisms in protection from phage infection[49–51] and a recent study reporting an accumulation of defence systems in phage-resistant *Pa* strains[52]. However, these findings are consistent with other studies that have likewise not identified roles for bacterial defence mechanisms in *Pa* resistance to lytic phages[21,53,54]. This discrepancy may be explained by high specificity of phage defence mechanisms to particular phages, which may not offer generalized protection. Alternatively, generalized protection may exist, but the presence of sophisticated phage strategies to counteract bacterial defence systems may confound its observation[9,23]. To this point, it is known that some "jumbo" phages such as OMKO1 can form a phage nucleusduring intracellular replication that can physically protect against DNA-targeting defence systems[40].

Interestingly, we observe that defence systems are associated with the number of temperate phages integrated in the bacterial genome. Two significant defence systems, PDC-202 and Helicase-DUF2290, exhibited a positive correlation with the number of phages. Conversely, two other systems, PDC-M61 and Cas type I-F1, showed a negative correlation. Defence mechanisms are often encoded in prophages, which could confer a competitive advantage to bacteria harboring temperate phages[55]. Conversely, other defence mechanisms may provide protection against temperate phages[56].

The findings presented here are specific to the experimental design and phages studied. Different approaches or experiments exploring the relationships and co-evolution between phages and hosts over an extended period, particularly those focusing on the development of phage resistance, may yield different outcomes, shown by a recent study suggested an accumulation of defence systems in phage-resistant *Pa* strains[52].

While Tn mutagenesis assays can identify genes linked to phage susceptibility, they do not reveal genes associated with phage resistance. A transposon insertion into such a gene (loss-of-function) would not confer protection against phage, making it impossible to study a connection with phage infection. Future studies could incorporate gain-of-function assays[57] or gene cloning for further investigation[54]. In contrast, the GWAS may reveal subtle genetic changes associated with phage susceptibility, making it a powerful tool for identifying single mutations that may confer bacterial resistance.

Padloc represents a robust tool for identifying bacterial defence systems within bacterial strains, being one of the most updated platforms[58]. However, it's important to acknowledge that the mere presence of a gene in the genome does not guarantee its expression and functionality, and the tool may not encompass all known defence systems, let alone undiscovered ones. Moreover, defence systems across bacterial species and strains are highly diverse[59]. This diversity, along with their potential interactions or analogies, may reduce the power to detect individual systems and their correlation with phage susceptibility. Nonetheless, Padloc remains the best choice for comprehensive screening, given the impracticality of manual identification.

In conclusion, this study identified genes and structural proteins crucial for phage susceptibility and resistance. Specifically, flagella were found to play a pivotal role in OMKO1 phage infection, while the O-antigen in lipopolysaccharide was identified as important for LPS-5 phage infection. Subsequent swimming assays confirmed these structures as receptors for their respective phages. Conversely, our data does not support existing paradigms regarding the central role of phage defence mechanisms in determining host range for lytic phages. These results may contribute to our understanding of the constraints of phage infection and could facilitate the development of phage therapy.

Method and Materials

Bacteriophages and *Pa*. The phages investigated in this study include the Myoviridae phages LPS-5 and OMKO1. LPS-5 is used in the Cystic Fibrosis Bacteriophage Study at Yale (CYPHY) (NCT04684641) [27], while OMKO1 (outer-membrane-porin M knockout dependent phage 1) was isolated at Yale University [26] (Table 3, Supplementary Figure 7).
PAO1 and the clinical *Pa* isolates used in this study were obtained from our research group (Table 4).

Table 3: Bacteriophages

Name	Family	Host	Origin
OMKO1 (outer-membrane-porin M knockout dependent phage 1)	Myoviridae	*Pseudomonas aeruginosa* PAO1	B. K. Chan et al., Yale University [26]
LPS-5	Myoviridae	*Pseudomonas aeruginosa* PAO1	B. K. Chan et al., Yale University [27]

Table 4: Bacterial strains

Strain	Species	Application
PAO1	*Pseudomonas aeruginosa*	Tn assay, experimental validation
80 clinical isolates	*Pseudomonas aeruginosa*	lytic plaque assay

Transposon mutagenesis assay. The creation of a transposon mutagenesis library was previously described by Larry Gallagher et al. in the Manoil group at the University of Washington.[60] Tn mutagenesis was performed via conjugation of the *Escherichia coli* SM10λpir/pIT2, a Tn5-derived transposon, followed by selection for *Pa* derivatives carrying the transposon tetracycline-resistance element. This results in a different transposon insertion and gene disruption in each mutant strain. The composition of transposon mutant pools was characterized using the Tn-seq circle method (35). The *Pa* library, along with the phages LPS-5 and OMKO1, underwent expansion and titration. For the assay, a bacterial concentration at least 1000 times greater than the number of unique mutants ($1x10^5$) was utilized, resulting in an inoculation of $1x10^8$ colony-forming units (cfu) in 25 ml of LB medium. The phages were added at two multiplicities of infection (MOI), 20 and 0.1, corresponding to $2x10^9$ and $1x10^7$, respectively plaque-forming units per milliliter of the medium (pfu/mL). Bacterial cultures were grown to an optical density (OD) of 0.2-0.4, for a duration of 30 minutes to 3 hours depending on the MOI, which is equivalent to 1-3 phage propagation cycles. Subsequently, the bacterial cultures were harvested and prepared for genomic DNA (gDNA) extraction. Transposon region amplification of the gDNA was conducted using the C-tailing method, a PCR reaction with one primer targeting a C-tail region near the 3' end of the transposon and the second primer complementary to bacterial genomic DNA. Following PCR Tn amplification, DNA was quantified to ensure equal DNA amounts for subsequent Tn-Seq protocol steps. This was followed by library preparation to add adapter sequences necessary for Illumina sequencing. Transposons were sequenced for distinct timepoints and conditions: before phage administration (T0), after killing assay with phage (T1P sequence condition at timepoint 1, see above for durations), and without phage (T1 condition). Reads were mapped to the bacterial genome and quantified. Abundant transposon counts indicated bacterial survival, suggesting that the disruption of the gene played a protective role against phage infection. This allowed the identification of genes crucial for phage infection. Conversely, minimal or absent transposon counts signified bacterial death despite the non-functioning gene and that the disrupted gene was not essential for phage infection.

Analysis. We first normalized the read counts, dividing the count of a particular gene under a specific condition (timepoint and phage condition) by the sum of all the reads for all the genes at that same timepoint and condition. Following normalization, the gene fitness score was computed by taking the

log2 of the normalized gene count at timepoint T1 under the specific phage condition, divided by the count of that gene at timepoint T0 (Equation (1)).

$$\text{gene fitness score} = log2\left(\frac{count_{gene,\ phage\ condition\ T1}}{count_{gene,\ T0}}\right) \quad (1)$$

We then performed a Fisher's test to identify genes significantly enriched in the Tn assay. The Fisher's exact test calculates the significance of the deviation from the null hypothesis from a contingency table of two categorical variables [61], in this case phage condition and time.

A functional enrichment analysis was performed using the enrichKEGG package [62] to explore these genes further and identify significantly enriched pathways (Table 5). Significant hits were assigned to classes of genes and pathways that were over-represented in the gene set, likely associated with the phage infection phenotype. For a more detailed examination of pathways, functional enrichment analysis using the PANTHER [63] program was then conducted. These two analytical methods use different databases where enrichKEGG focuses on pathway enrichment analysis using the KEGG database and PANTHER offers a broader spectrum of functional analysis tools, including pathway enrichment along with gene ontology and protein interaction analysis.

Table 5: Statistical and analytical tools

Tool	Origin	Application
Fisher's Exact Test for Count Data	R. A. Fisher [61]	Tn assay
enrichKEGG	G. Yu et al. [62]	Functional enrichment analysis
PANTHER	H. Mi et al. [63]	Functional enrichment analysis
Genome-Wide Association Study (GWAS) / De Bruijn Genome-Wide Association Study (DBGWAS)	M. Jaillard et al. [64]	GWAS with lytic plaque assay
GraphPad Prism Version 7	GraphPad Prism	Suppression Ratio calculation
Blast	NCBI [65]	Mutations in flagella and LPS associated genes
Mafft	Katoh K. et al. [66]	Sequence alignments
Cons, EMBOSS	Rice P. et al. [67]	Consensus sequences
Prokaryotic Antiviral Defence LOCator (Padloc)	L. J Payne et al. [58]	Bacterial defence systems
Wilcoxon signed-rank test	Kurt Hornik [68]	Bacterial defence systems, single system analysis
Generalized Linear Model (glm)	Simon Davies [69]	Bacterial defence systems, all systems
R Version 4.3 and RStudio	R and RStudio	Analysis, graphs
BioRender	BioRender [70]	Schematics

Suppression Assay. Cultures from frozen stock were initially incubated overnight at 37°C with shaking at 250 rpm. Following this, overnight cultures of bacterial strains were diluted 1:200 with LB medium

(Table 6) and regrown for 2-3 hours until reaching an OD600 of approximately 0.1-0.2. Subsequently, this culture was diluted 1:10 into the wells of a 96-well plate, and phage was added to achieve a MOI of 100, resulting in a total volume of 150 µl per well. The 96-well plate was then incubated at 37°C with shaking for 30 hours, during which the OD600 was measured every 20 minutes using an automated spectrophotometer (Biotek microplate reader). All growth curves were adjusted by subtracting the background curve (LB medium with phage buffer at a concentration of 1 mM MgSO4, 4 mM CaCl2, 50 mM Tris-HCl (pH=7.8), 6 g/L NaCl, and 1 g/L gelatin). The Suppression Ratio, expressed as a percentage, was calculated using GraphPad Prism Version 7.0 software. This ratio was defined as the area under the curve (AUC) for the non-phage-treated condition minus the AUC for the phage-treated condition, divided by the AUC of the non-treated condition.

Table 6: Media, Buffers, Chemicals

Media, Buffer, Chemical	Ingredients	Concentration
LB Agar for Swimming Assay	Agar Tryptone medium	0.3% 1%
LB Agar for LPS/O-AG Assay	LB Agar TSB medium Congo red Coomassie brilliant blue	 1% 1% 40 mg/L 20mg/L
Phage buffer	MgSO4 CaCl2 Tris-HCl (pH=7.8) NaCl Gelatin	1 mM 4 mM 50 mM 6 g/L 1 g/L

Swimming assay. Following a standardized protocol[71], overnight cultures were initially grown and subsequently diluted before regrowth to an OD of 0.1-0.2. The bacterial suspension was then transferred onto agar plates via puncturing with a pipette tip. These agar plates were prepared using 1% tryptone medium supplemented with 0.3% agar. After incubation for 24 hours at 37°C, the growth zones were measured. The experiment was conducted with a minimum of 5 repetitions.

LPS/O-AG assay. Following an established protocol[44], 1µl of overnight culture of clinical isolates were spotted onto agar plates containing 1% TSB medium fortified with 40 mg/L Congo red and 20 mg/L Coomassie brilliant blue dyes and solidified with 1% agar. Colony biofilms were grown for 4 days at 25°C before images were taken and the morphology analysed (Supplementary Figure 8).

Whole genome sequencing and assembly. We collected Pa isolates from sputum samples from individuals with CF and banked them with patient consent under IRB #11197, approved by the Stanford University Institutional Review Board. DNA was extracted using the DNA Easy Kit (Qiagen, 69504, Hilden, Germany) and sequenced with Illumina. We trimmed raw reads using trimmomatic[73] and then assembled them with SPAdes using –isolate and --cov-cutoff auto[74].

Mutant calling. Flagella genes and LPS biosynthetic gene sequences (Supplementary Figure) were downloaded from the Pseudomonas genome database[72]. These sequences were blasted against the genomes of the clinical isolates using the ncbi-blast software[65]. Hits were then aligned using mafft[66]. To identify non-synonymous mutations, aligned sequences over a specific length (>20% of the total sequence, typically around >400 bp) were translated. Subsequently, each amino acid was compared to the reference sequence used for the blast analysis. Changes in amino acids were documented, including the amino acid position and the specific alteration. For sequences exhibiting high diversity (sequence

similarity < 90%), consensus sequences for both resistant and susceptible strains were generated. Consensus sequences for each variant were derived using the cons function from the European Molecular Biology Open Software Suite (EMBOSS[67]).

GWAS with lytic plaque assay. A lytic plaque assay was conducted to determine which clinical Pa strains were susceptible to the phages OMKO1 and LPS-5. This phenotypic data, combined with the whole-genome sequencing of the clinical isolates, was used in a Genome-Wide Association Study (GWAS) to identify genes associated with either phage susceptibility or resistance.

Experiments. In the lytic plaque assay, 80 clinical Pa strains were plated on rectangular LB agar plates, followed by the addition of drops of distinct phages in different dilutions (dilution factors: 0, 1, 3, 5, 7). Each experiment was repeated three times and the phages tested were OMKO1 and LPS-5. The plates were then incubated to allow phage infection and plaque formation.

Analysis. The assessment of plaques involved several parameters (Equation (2)), including single plaque status (SPS), plaque score of the sample (PS) and reference (RS), and inhibition score (IS). SPS was assigned a value of 1 if single plaque resolution was observed at any phage dilution, and 0 otherwise. When SPS was 0, PS was also assigned 0, however, if SPS was 1, its value was determined by the dilution factor with single plaque resolution. RS represented the dilution factor of the reference strain when SPS was 1, assuming a nonzero plaque score for the reference strain. In cases where SPS was 0, IS was set to the highest dilution factor with signs of bacterial growth inhibition. These parameters collectively contributed to the derived score for each clinical isolate, ranging from 0 to 2. Scores between 0 and 1 indicate phage resistance or inhibition of bacterial growth, while scores between 1 and 2 indicate phage susceptibility. This phenotypic data, combined with the genome sequences of the clinical isolates as genotypic data, was used in the GWAS to identify genes associated with either phage susceptibility or resistance.

$$\boldsymbol{Score = SPS + SPS * (1 - (RS - PS) * 0.1) + \frac{IS}{RS}}$$

SPS: Single plaque status (0 or 1)

PS: Plaque score (0,1,3,5 or 7)

RS: Plaque score for reference strain (0,1,3,5 or 7)

IS: Inhibition score (0,1,3,5 or 7)

(2)

We performed a De Bruijn Genome-Wide Association Study (DBGWAS). A DBGWAS requires genome assemblies and phenotypic data for a panel of bacterial strains as input and outputs phenotype-associated genetic events and an interactive interface featuring regions of the DBG surrounding statistically significant nodes.

Given the numerous genes identified by the GWAS in association with phage infection, a functional enrichment analysis was conducted to identify enriched pathways using the enrichKEGG package. Significant hits are assigned to classes of genes and entire pathways that are over-represented in the gene set associated with the phage infection phenotype.

Bacterial defence systems and lytic phage infection. The genomes of the clinical isolates were screened for bacterial defence systems using the Prokaryotic Antiviral Defence LOCator (Padloc).[58] We assessed the association of each system with lytic scores using a Generalized Linear Model (GLM),

which was only fitted to systems that were significantly associated with phage resistance or susceptibility, as determined by a Wilcoxon signed-rank test. [75] P-values from the Wilcoxon test were adjusted for multiple testing using a Bonferroni correction (each p-value was multiplied by the total number of tests conducted, corresponding to the number of defence systems evaluated). Any corrected p-value exceeding 1 was set to 1. Since no defence systems showed significance in the Wilcoxon test, the systems that exhibited significance prior to p-value correction were selected for inclusion in the GLM [69]. The GLM was fitted with a binomial distribution, and the AIC criterion [76] was employed to compare the fit of different distributions and determine the optimal number of defence systems to include. Additionally, residual diagnostics were performed using the DHARMa package [77] to confirm the goodness of fit of the model.

Bacterial defence systems and temperate phages. We followed the steps described above using the number of temperate phages in the bacterial genome as a response variable. We identified temperate phages using VIBRANT and blast and looked for bacterial defence systems using Padloc. The relationship between each defence system and the number of temperate phages was individually analysed using a Wilcoxon test. Subsequently, significant predictors were included in a generalized linear model with a Poisson distribution to evaluate the association between these defence mechanisms and the number of temperate phages.

Data and code availability. All bacterial strains, bacteriophages, materials, and experimental data are available upon request. All detailed codes used for analysis are available upon request.

Acknowledgments
We extend our heartfelt gratitude to all members of the Bollyky Laboratory for insightful discussions and support. We thank the members of Felix Biotechnology, Inc (San Francisco, CA) for the data from the Transposon mutagenesis experiment and lytic plaque assay. JDA and PET acknowledge funding support from a research grant award by Howard Hughes Medical Institute.

Authors and Contributors
P.L.B., J.D.P. and D.M.M. conceptualized the main idea of this research project. D.M.M. performed the majority of the experiments and analysis. J.D.P. assembled and processed the bacterial genomes and identified temperate phages. P.L.B., L.A.G and J.D.P. provided feedback on the results. D.M.M. wrote the paper. P.L.B., L.A.G, J.D.P., M.K.K and D.M.M. contributed to the revision of the paper. M.K.K and J.D.A. supported the experimental validation and Maryam Hajfathalian[1] provided the TEM pictures. D.M.M. and B.T. created the LPS schematic. E.B.B. collected and banked the clinical isolates and contributed to revisions of the manuscript. R.M. (Co-Founder & CEO of Felix Biotechnology) provided the Transposon mutagenesis experiment and lytic plaque assay.

Competing interests
The authors declare no competing interests.

Main Figures

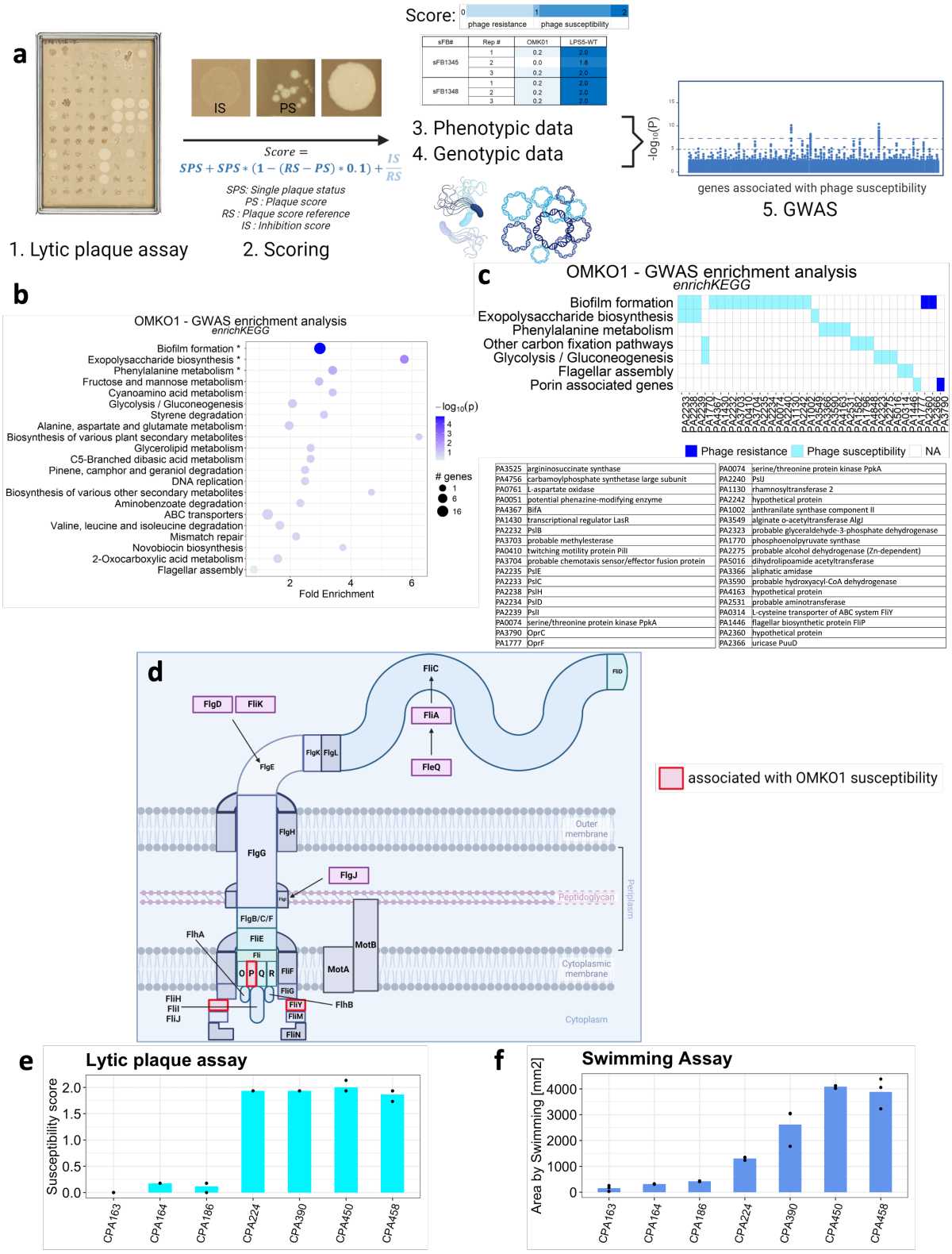

sFB#	Rep #	OMK01	LPS5-WT
sFB1345	1	0.2	2.0
	2	0.0	1.8
	3	0.2	2.0
sFB1348	1	0.2	2.0
	2	0.2	2.0
	3	0.2	2.0

PA3525	argininosuccinate synthase
PA4756	carbamoylphosphate synthetase large subunit
PA0761	L-aspartate oxidase
PA0051	potential phenazine-modifying enzyme
PA4367	BifA
PA1430	transcriptional regulator LasR
PA2232	PslB
PA3703	probable methylesterase
PA0410	twitching motility protein PilI
PA3704	probable chemotaxis sensor/effector fusion protein
PA2235	PslE
PA2233	PslC
PA2238	PslH
PA2234	PslD
PA2239	PslI
PA0074	serine/threonine protein kinase PpkA
PA3790	OprC
PA1777	OprF

PA0074	serine/threonine protein kinase PpkA
PA2240	PslJ
PA1130	rhamnosyltransferase 2
PA2242	hypothetical protein
PA1002	anthranilate synthase component II
PA3549	alginate o-acetyltransferase AlgJ
PA2323	probable glyceraldehyde-3-phosphate dehydrogenase
PA1770	phosphoenolpyruvate synthase
PA2275	probable alcohol dehydrogenase (Zn-dependent)
PA5016	dihydrolipoamide acetyltransferase
PA3366	aliphatic amidase
PA3590	probable hydroxyacyl-CoA dehydrogenase
PA4163	hypothetical protein
PA2531	probable aminotransferase
PA0314	L-cysteine transporter of ABC system FliY
PA1446	flagellar biosynthetic protein FliP
PA2360	hypothetical protein
PA2366	uricase PuuD

Figure 1: A GWAS study reveals genes associated with susceptibility to OMKO1. a, During the lytic plaque assay, plaques assessment included single plaque status, plaque score of the sample and reference, and inhibition score. These factors collectively contributed to the derived score, which was used alongside genomic data for the GWAS. **b,** Each bubble represents a specific functional category, with the size of the bubble indicating the number of associated genes, and the color intensity reflecting the statistical significance level of the enrichment. Significant pathways are labelled with a star. Notably, the most significant pathway identified is Biofilm formation. Additionally, the pathway for flagellar

assembly is also detected in the analysis. **c,** This heatmap illustrates the categorization of genes on the x-axis into distinct functional groups on the y-axis. The color scheme distinguishes genes associated with phage susceptibility, depicted in bright blue, from those linked to phage resistance, represented in dark blue. Notably, two genes within the flagellar assembly pathway can be identified, revealing an association with phage susceptibility. Two porin genes could be identified in the dataset. **d,** Schematic representation of flagella and essential structural proteins. Proteins identified through the above described experiments as associated with OMKO1 phage susceptibility are highlighted in red. **e,** Of the 80 clinical *Pa* isolates, only 4 were susceptible to OMKO1 shown by the high susceptibility score from the lytic plaque assay. This is consistent with the well-described loss of a functional flagella associated with *Pa* colonization in pwCF. **f,** With a swimming assay, described before, we could perfectly show that flagella functionality explains the susceptibility pattern of OMKO1 of the lytic plaque assay.

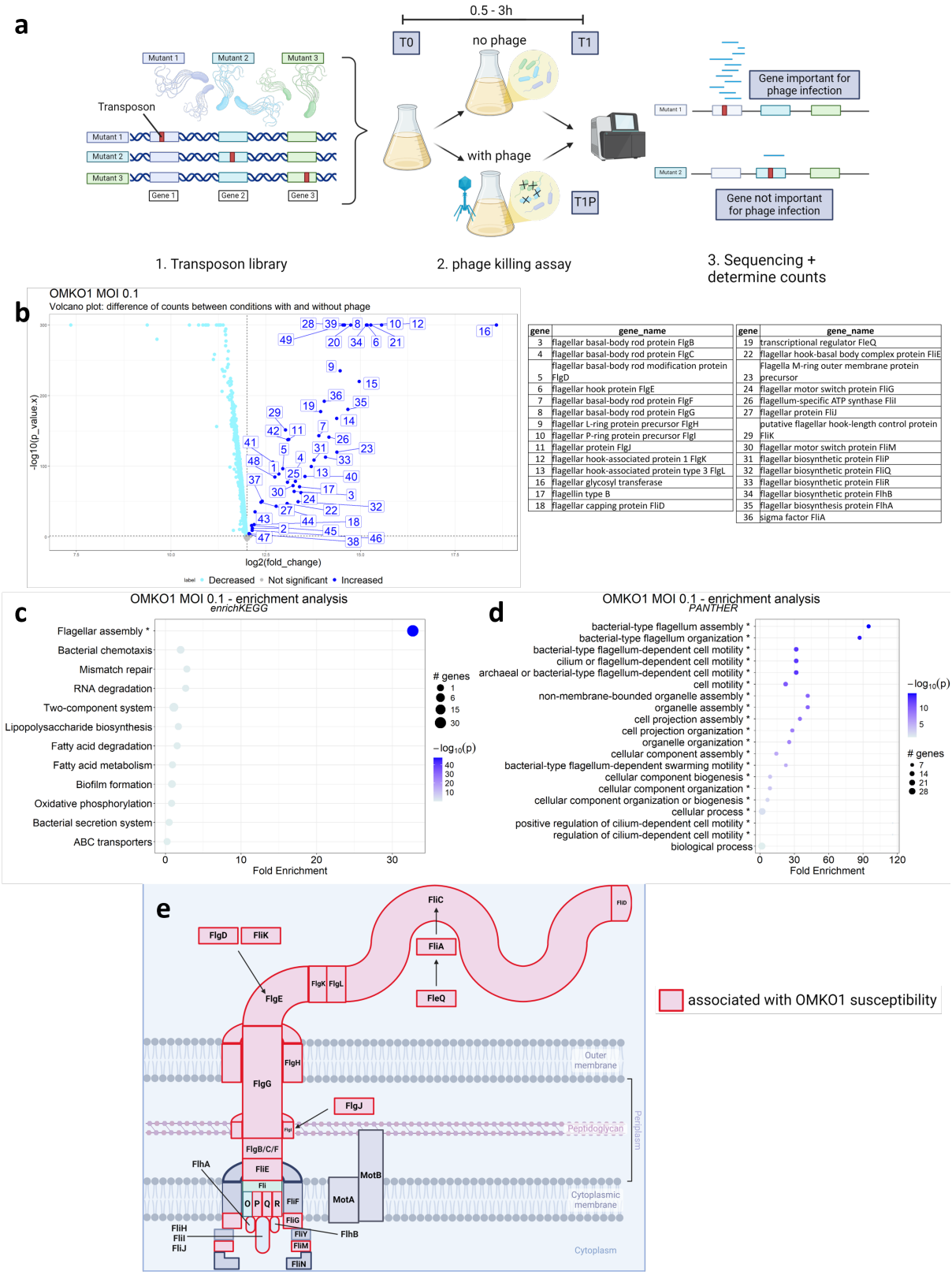

gene	gene_name
3	flagellar basal-body rod protein FlgB
4	flagellar basal-body rod protein FlgC
5	flagellar basal-body rod modification protein FlgD
6	flagellar hook protein FlgE
7	flagellar basal-body rod protein FlgF
8	flagellar basal-body rod protein FlgG
9	flagellar L-ring protein precursor FlgH
10	flagellar P-ring protein precursor FlgI
11	flagellar protein FlgJ
12	flagellar hook-associated protein 1 FlgK
13	flagellar hook-associated protein type 3 FlgL
16	flagellar glycosyl transferase
17	flagellin type B
18	flagellar capping protein FliD

gene	gene_name
19	transcriptional regulator FleQ
22	flagellar hook-basal body complex protein FliE
23	Flagella M-ring outer membrane protein precursor
24	flagellar motor switch protein FliG
26	flagellum-specific ATP synthase FliI
27	flagellar protein FliJ
29	putative flagellar hook-length control protein FliK
30	flagellar motor switch protein FliM
31	flagellar biosynthetic protein FliP
32	flagellar biosynthetic protein FliQ
33	flagellar biosynthetic protein FliR
34	flagellar biosynthetic protein FlhB
35	flagellar biosynthesis protein FlhA
36	sigma factor FliA

Figure 2: Transposon Mutagenesis Experiments show that Flagella-Associated Genes are required for OMKO1 Phage Infection. a, In the transposon mutagenesis library, a distinct gene in each mutant strain was disrupted via a transposon insertion. Following co-cultivation with phages, transposons were sequenced and quantified. Abundant transposon counts indicated bacterial survival, suggesting that the disrupted gene played a protective role against phage infection. This allowed the identification of genes crucial for phage infection. Conversely, minimal or absent transposon counts signified bacterial death despite the non-functioning gene. This observation indicated that the disrupted

gene was not essential for phage infection. **b,** This volcano plot highlights genes with a significant difference in counts (fold change) between conditions with and without OMKO1 phage at MOI 20. Each point represents a gene, with the x-axis showing the log2 fold change and the y-axis representing statistical significance. Significant increase in gene count is showed in dark blue, significant decrease in bright blue and non significant genes in gray. Notably, a majority of genes showing a significant increase in counts in the presence of phage, indicative of their importance in phage infection, are associated with flagella for the phage OMKO1. (The complete list of significant genes can be found in Supplementary Figure 2) **c,** This plot visually summarizes functional enrichment analysis results conducted with enrichKEGG, where each bubble represents a functional category. The size of each bubble corresponds to the number of associated genes, and the colour intensity indicates the significance level. Significant pathways are labelled with a star. Specifically for the phage OMKO1 at MOI 20, significant functional categories are linked to flagella assembly. **d,** Functional enrichment analysis using PANTHER enables a more detailed examination. Significant functional categories are associated with flagellum-dependent cell motility and flagellum assembly, particularly for the phage OMKO1. **e,** Schematic representation of flagella and essential structural proteins. Proteins identified through Tn mutagenesis experiments as associated with OMKO1 phage susceptibility are highlighted in red.

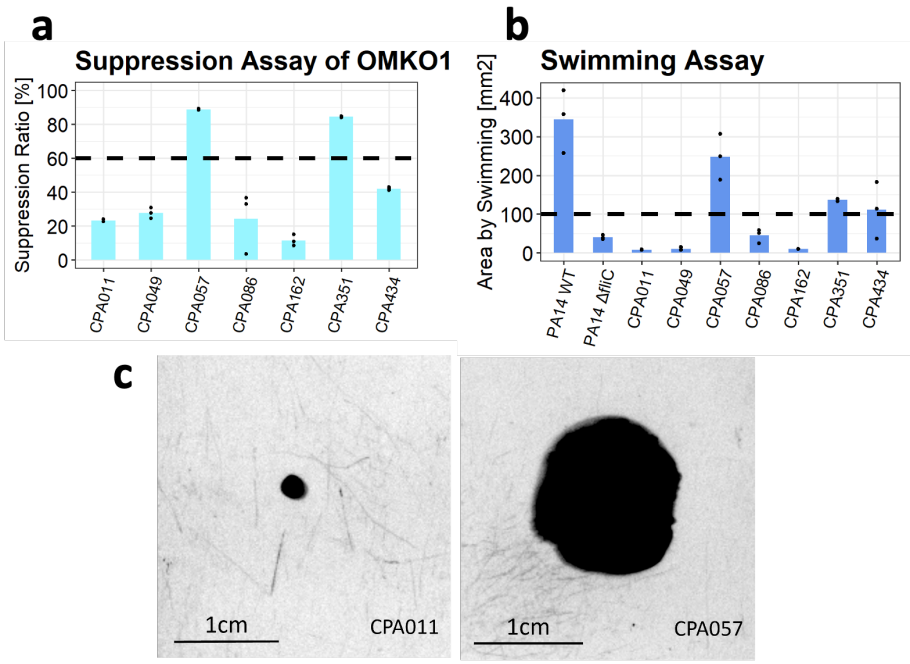

Figure 3: The presence of a functional bacterial flagella is associated with susceptibility to OMKO1 predation. a, Phage suppression (Suppression ratio) was assessed for CPA. A value above the threshold indicates susceptibility to the OMKO1 phage, while values below indicate phage resistance. The suppression ratio was calculated as the area under the curve (AUC) for the non-phage-treated condition minus the phage-treated condition, divided by the AUC of the non-treated sample. **b,** The area covered by swimming was measured for various clinical Pseudomonas isolates (CPA). Growth areas similar to those of the *ΔfliC* strain indicate non-functional flagella, while swimming behavior comparable to that of the WT strain indicates functional flagella. **c,** Large colony growth area indicates the presence functional flagella allowing swimming (CPA057), whereas small colony growth area indicates non-functional flagella (CPA011).

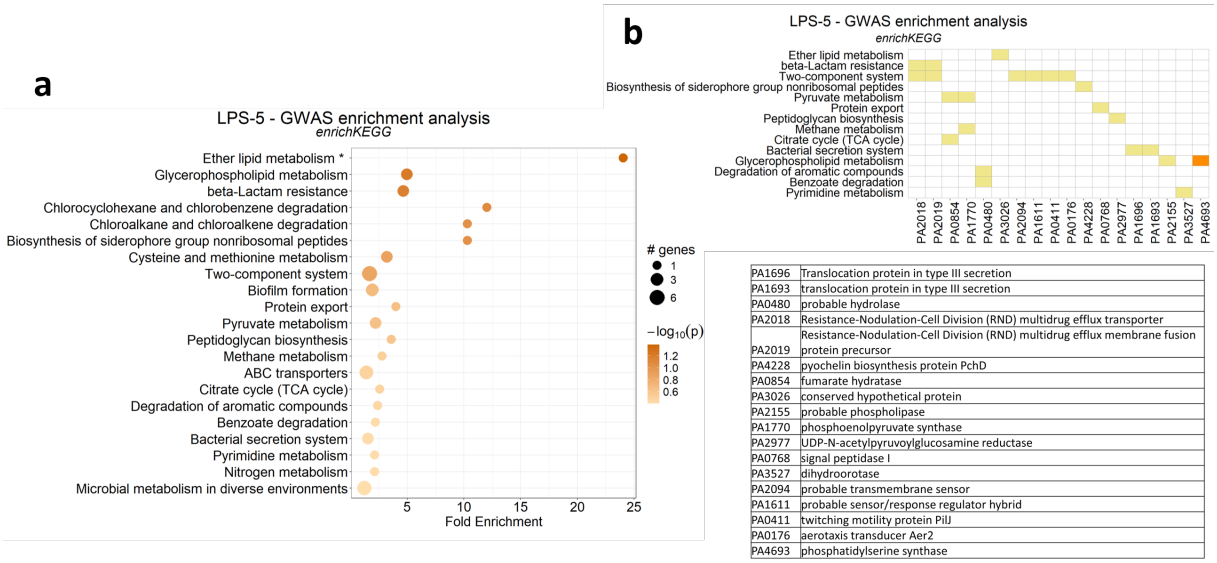

PA1696	Translocation protein in type III secretion
PA1693	translocation protein in type III secretion
PA0480	probable hydrolase
PA2018	Resistance-Nodulation-Cell Division (RND) multidrug efflux transporter
PA2019	Resistance-Nodulation-Cell Division (RND) multidrug efflux membrane fusion protein precursor
PA4228	pyochelin biosynthesis protein PchD
PA0854	fumarate hydratase
PA3026	conserved hypothetical protein
PA2155	probable phospholipase
PA1770	phosphoenolpyruvate synthase
PA2977	UDP-N-acetylpyruvoylglucosamine reductase
PA0768	signal peptidase I
PA3527	dihydroorotase
PA2094	probable transmembrane sensor
PA1611	probable sensor/response regulator hybrid
PA0411	twitching motility protein PilJ
PA0176	aerotaxis transducer Aer2
PA4693	phosphatidylserine synthase

Figure 4: GWAS with lytic plaque assay. a, With the results of the GWAS, a comprehensive functional enrichment analysis was conducted and illustrated in the bubble graph. Each bubble represents a specific functional category, with the size of the bubble indicating the number of associated genes, and the color intensity reflecting the statistical significance level of the enrichment. Significant pathways are labelled with a star. Different metabolic pathways are significantly enriched and relevant to phage susceptibility. **b,** This heatmap illustrates the categorization of genes on the x-axis into distinct functional groups on the y-axis. The color scheme distinguishes genes associated with phage susceptibility, depicted in yellow, from those linked to phage resistance, represented in orange. This facilitates the identification of genes within pathways and demonstrates whether these pathways are linked either to phage resistance or susceptibility.

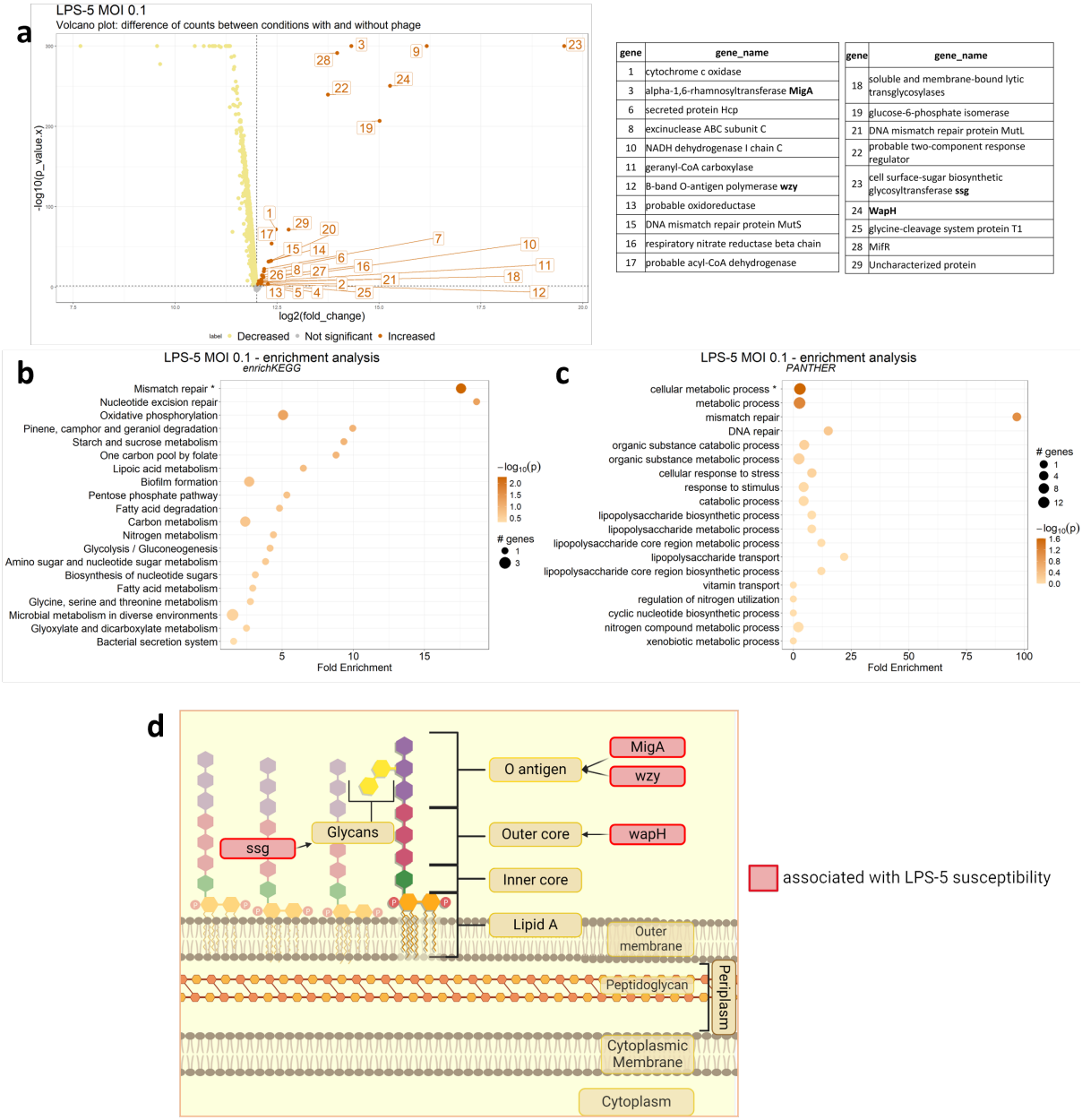

gene	gene_name
1	cytochrome c oxidase
3	alpha-1,6-rhamnosyltransferase **MigA**
6	secreted protein Hcp
8	excinuclease ABC subunit C
10	NADH dehydrogenase I chain C
11	geranyl-CoA carboxylase
12	B-band O-antigen polymerase **wzy**
13	probable oxidoreductase
15	DNA mismatch repair protein MutS
16	respiratory nitrate reductase beta chain
17	probable acyl-CoA dehydrogenase

gene	gene_name
18	soluble and membrane-bound lytic transglycosylases
19	glucose-6-phosphate isomerase
21	DNA mismatch repair protein MutL
22	probable two-component response regulator
23	cell surface-sugar biosynthetic glycosyltransferase **ssg**
24	**WapH**
25	glycine-cleavage system protein T1
28	MifR
29	Uncharacterized protein

Figure 5: Identification of LPS-Associated Genes Crucial for LPS-5 Phage Infection through Transposon Mutagenesis Experiments. a, This volcano plot highlights genes with a significant difference in counts (fold change) between conditions with and without LPS-5 phage at MOI 20. Each point represents a gene, with the x-axis showing the log2 fold change and the y-axis representing statistical significance. Significant increase in gene count is showed in orange, significant decrease in yellow and non significant genes in gray. Notably, several genes showing a significant increase in counts in the presence of phage, indicative of their importance in phage infection, are associated with LPS. (The complete list of significant genes can be found in Supplementary Figure .) **b,** This plot visually summarizes functional enrichment analysis results conducted with enrichKEGG, where each bubble represents a functional category. The size of each bubble corresponds to the number of associated genes, and the colour intensity indicates the significance level. Significant pathways are labelled with a star. **c,** Functional enrichment analysis using PANTHER enables a more detailed examination. Several functional categories are associated with LPS and LPS biosynthesis, particularly for the phage LPS. **d,** Schematic representation of LPS and related pathways. Proteins identified through Tn mutagenesis experiments as associated with LPS-5 phage susceptibility are highlighted in red.

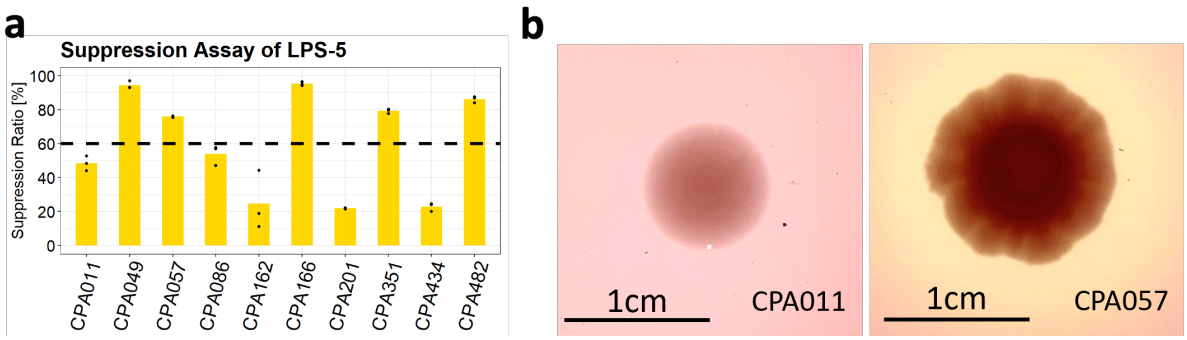

Figure 6: Experimental validation of O-antigen/LPS as the receptor for LPS-5. a, Phage suppression (Suppression ratio) was assessed for clinical CPA. A value above the treshold indicates susceptibility to the LPS-5 phage, while values below indicate phage resistance. The suppression ratio was calculated as the area under the curve for the non-phage-treated condition minus the phage-treated condition, divided by the AUC of the non-treated sample. **b,** Colony morphology displaying rugae indicates the presence of LPS containing O-antigen (O-AG), whereas smooth colonies lacking rugae suggest mutations in the O-AG within the LPS.

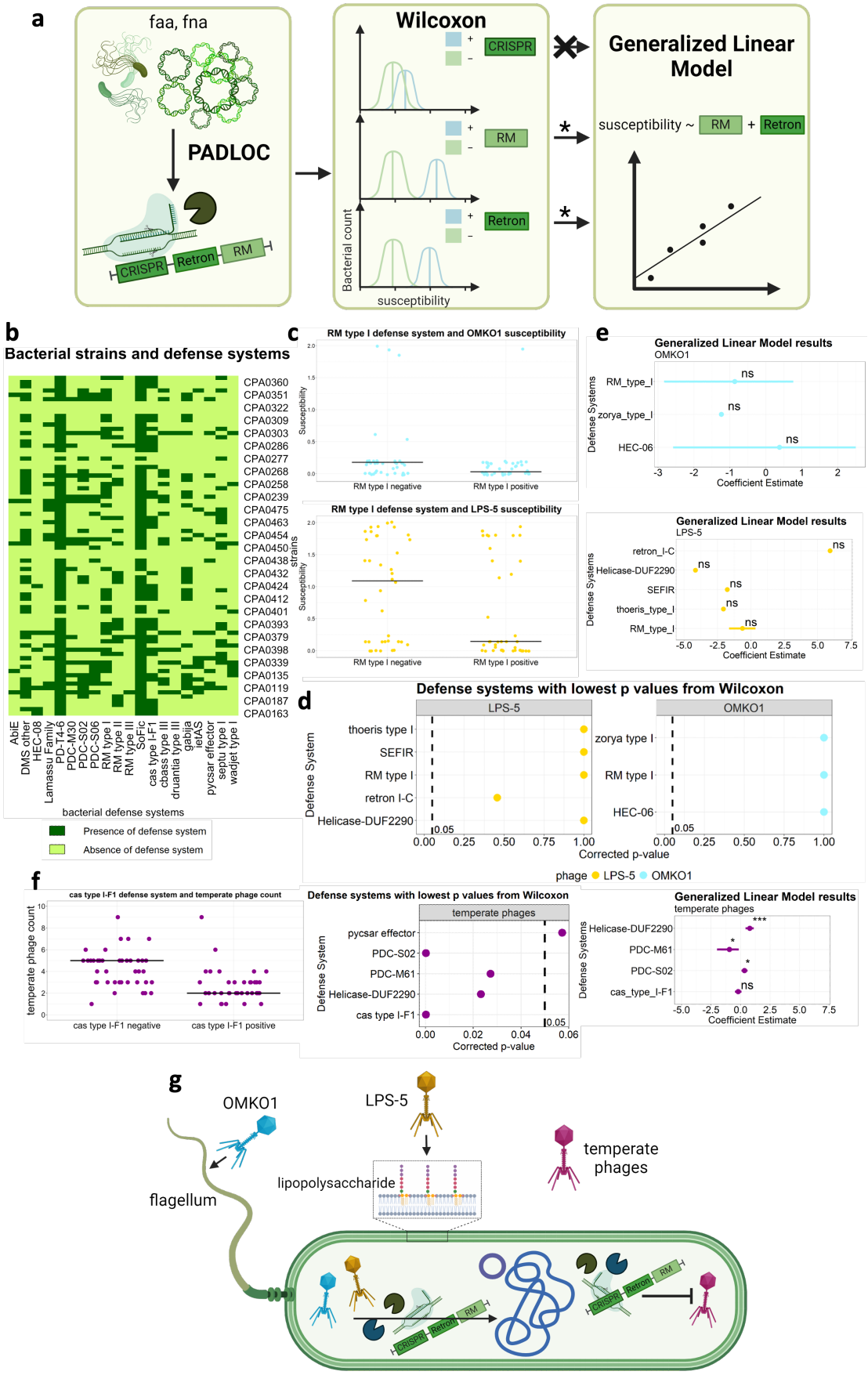

Figure 7: Presence of bacterial defence systems is not associated with lytic phage susceptibility. a, Defence System Analysis Workflow. Clinical isolates were screened for defence systems using the Prokaryotic Antiviral Defence LOCator (Padloc). Pre-selection of defence systems was conducted via a

Wilcoxon signed-rank test, followed by their inclusion in a generalized linear model to assess potential associations between the presence or absence of these defence mechanisms and phage susceptibility. **b,** Presence or absence of bacterial defence systems across bacterial strains. On the x-axis are the identified defence systems, while the y-axis represents individual bacterial strains. Presence or absence of a defence system is represented in colours. **c,** Phage susceptibility for isolates with and without RM Type I. Each point represents one bacterial strain grouped into RM type I negative and positive categories. The median is represented by the horizontal line. The first plot illustrates the data for OMKO1, while the second plot includes all data points for LPS-5. **d,** Wilcoxon Results. The plot illustrates the defence systems with the lowest p-values against their corrected p-values, indicating that none of the p-values fall below the significance threshold of 0.05 for any phage **e,** Whisker Plot of the GLM. The defence systems identified in the Wilcoxon analysis were incorporated into a Generalized Linear Model (GLM), demonstrating that none of the systems are significantly associated with OMKO1 susceptibility or LPS-5 susceptibility. Defence systems are plotted against their coefficient estimates, indicating their non-significance (ns). **f,** Bacterial defence systems are associated with the number of temperate phages in the bacterial genome. Similar to the previous analysis, we first investigated the association between the count of temperate phages and the presence of defence systems using a Wilcoxon test, followed by a GLM analysis. **g,** Concluding Schematic. This study suggests that receptors alone determine the host range of lytic phages. We identified the flagellum as a receptor of OMKO1 and lipopolysaccharide as the receptor of LPS-5. Although no significant relationship was found between bacterial defence systems and lytic phage infection, defence mechanisms may play a role in protecting against temperate phages.

Supplementary Figures

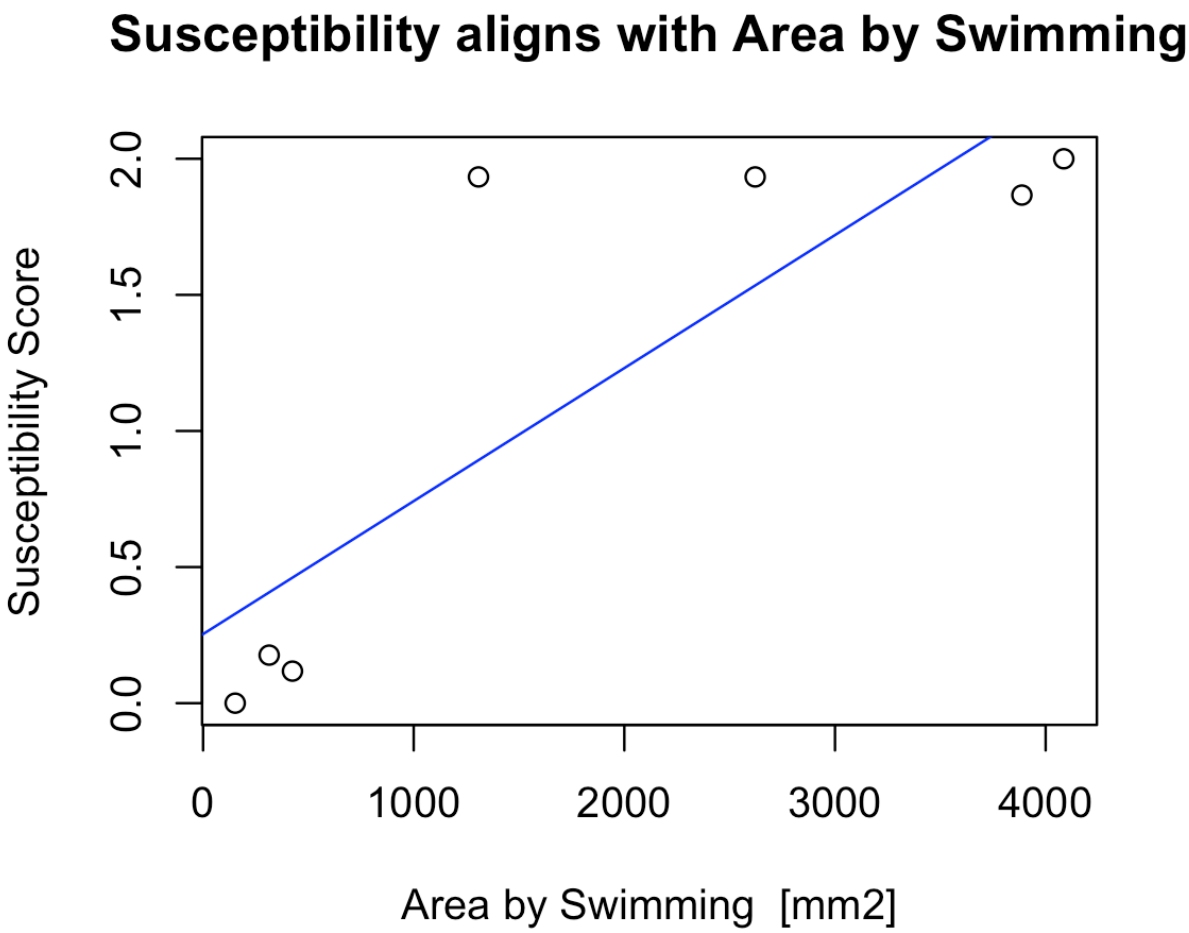

Supplementary Figure 1: Susceptibility Score plotted against the Area by Swimming, indicative of flagellar functionality. The model fit is shown in blue.

a

gene	gene name
1	hypothetical protein
2	methyltransferase PilK
3	flagellar basal-body rod protein FlgB
4	flagellar basal-body rod protein FlgC
5	flagellar basal-body rod modification protein FlgD
6	flagellar hook protein FlgE
7	flagellar basal-body rod protein FlgF
8	flagellar basal-body rod protein FlgG
9	flagellar L-ring protein precursor FlgH
10	flagellar P-ring protein precursor FlgI
11	flagellar protein FlgJ
12	flagellar hook-associated protein 1 FlgK
13	flagellar hook-associated protein type 3 FlgL
14	hypothetical protein
15	hypothetical protein
16	flagellar glycosyl transferase
17	flagellin type B
18	flagellar capping protein FliD
19	transcriptional regulator FleQ
20	two-component sensor
21	two-component response regulator
22	flagellar hook-basal body complex protein FliE
23	Flagella M-ring outer membrane protein precursor
24	flagellar motor switch protein FliG
25	probable flagellar assembly protein
26	flagellum-specific ATP synthase FliI
27	flagellar protein FliJ
28	cytochrome o ubiquinol oxidase subunit II
29	putative flagellar hook-length control protein FliK
30	flagellar motor switch protein FliM
31	flagellar biosynthetic protein FliP
32	flagellar biosynthetic protein FliQ
33	flagellar biosynthetic protein FliR
34	flagellar biosynthetic protein FlhB
35	flagellar biosynthesis protein FlhA
36	sigma factor FliA
37	probable acyl-CoA dehydrogenase
38	conserved hypothetical protein
39	hypothetical protein
40	hypothetical protein
41	DNA mismatch repair protein MutS
42	probable secretion protein
43	lipopolysaccharide biosynthetic protein LpxO1
44	probable rRNA methylase
45	exoribonuclease RNase R
46	probable transcriptional regulator
47	probable secretion pathway ATPase
48	CbcW
49	hypothetical protein

b

gene	gene name
1	hypothetical protein
2	L-aspartate oxidase
3	hypothetical protein
4	flagellar basal-body rod protein FlgB
5	flagellar basal-body rod protein FlgC
6	flagellar basal-body rod modification protein FlgD
7	flagellar hook protein FlgE
8	flagellar basal-body rod protein FlgF
9	flagellar basal-body rod protein FlgG
10	flagellar L-ring protein precursor FlgH
11	flagellar P-ring protein precursor FlgI
12	flagellar protein FlgJ
13	flagellar hook-associated protein 1 FlgK
14	flagellar hook-associated protein type 3 FlgL
15	hypothetical protein
16	hypothetical protein
17	flagellar glycosyl transferase
18	flagellin type B
19	flagellar capping protein FliD
20	transcriptional regulator FleQ
21	two-component sensor
22	two-component response regulator
23	flagellar hook-basal body complex protein FliE
24	Flagella M-ring outer membrane protein precursor
25	flagellar motor switch protein FliG
26	probable flagellar assembly protein
27	flagellum-specific ATP synthase FliI
28	flagellar protein FliJ
29	glutathione-regulated potassium-efflux system protein KefB
30	cytochrome o ubiquinol oxidase subunit II
31	putative flagellar hook-length control protein FliK
32	flagellar motor switch protein FliM
33	flagellar biosynthetic protein FliP
34	flagellar biosynthetic protein FliQ
35	flagellar biosynthetic protein FliR
36	flagellar biosynthetic protein FlhB
37	flagellar biosynthesis protein FlhA
38	sigma factor FliA
39	probable acyl-CoA dehydrogenase
40	hypothetical protein
41	hypothetical protein
42	DNA mismatch repair protein MutS
43	hypothetical protein
44	probable secretion protein
45	RNA polymerase sigma-54 factor
46	type 4 fimbrial biogenesis protein PilX
47	type 4 fimbrial biogenesis protein PilY1
48	probable rRNA methylase
49	DNA mismatch repair protein MutL
50	Type 4 fimbrial biogenesis outer membrane protein PilQ precursor
51	type 4 fimbrial biogenesis protein PilM
52	CbcW
53	hypothetical protein
54	thiol:disulfide interchange protein DsbA
55	hypothetical protein

Supplementary Figure 2: Full legend to the volcano plots of OMKO1 at MOI 0.1 (a.) and MOI20 (b.).

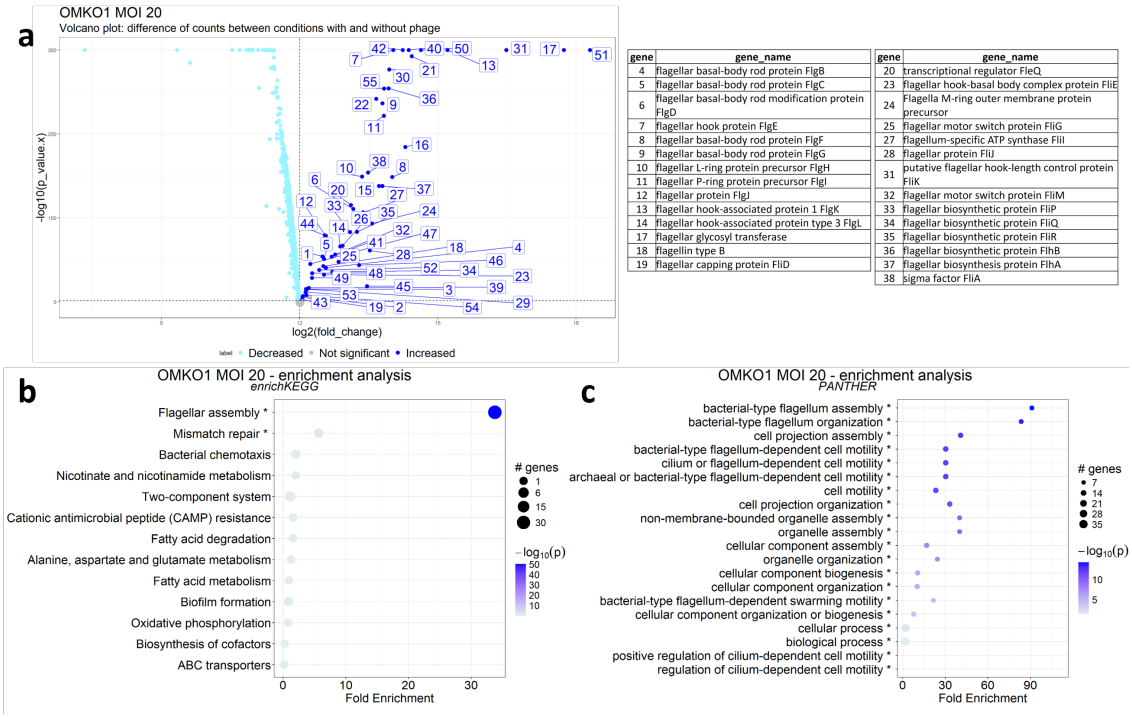

gene	gene_name
4	flagellar basal-body rod protein FlgB
5	flagellar basal-body rod protein FlgC
6	flagellar basal-body rod modification protein FlgD
7	flagellar hook protein FlgE
8	flagellar basal-body rod protein FlgF
9	flagellar basal-body rod protein FlgG
10	flagellar L-ring protein precursor FlgH
11	flagellar P-ring protein precursor FlgI
12	flagellar protein FlgJ
13	flagellar hook-associated protein 1 FlgK
14	flagellar hook-associated protein type 3 FlgL
17	flagellar glycosyl transferase
18	flagellin type B
19	flagellar capping protein FliD

gene	gene_name
20	transcriptional regulator FleQ
23	flagellar hook-basal body complex protein FliE
24	Flagella M-ring outer membrane protein precursor
25	flagellar motor switch protein FliG
27	flagellum-specific ATP synthase FliI
28	flagellar protein FliJ
31	putative flagellar hook-length control protein FliK
32	flagellar motor switch protein FliM
33	flagellar biosynthetic protein FliP
34	flagellar biosynthetic protein FliQ
35	flagellar biosynthetic protein FliR
36	flagellar biosynthetic protein FlhB
37	flagellar biosynthesis protein FlhA
38	sigma factor FliA

Supplementary Figure 3: a, This volcano plot describes genes with a significant difference in counts (fold change) between conditions with and without OMKO1 phage at MOI 0.1. Dark blue signifies a significant increase in gene counts, bright blue stands for a significant decrease, and gray represents non-significant genes. **b,** Similar to the previous functional analysis plots, this section summarizes the functional enrichment analysis results for the OMKO1 phage at MOI 0.1 with enrichKEGG. **c,** Key functional categories identified through the more detailed PANTHER analysis are linked to flagellum-dependent cell motility and flagellum assembly, providing insights into the enriched functions specific to the OMKO1 phage.

Supplementary Figure 4: Consensus sequences

Start codon	M
Stop codon	*
No base/sequence identified in blast	-

***FliC* consensus sequence of resistant strains**

```
MALTVNTNIASLNTQRNLNASSNDLNTSLQRLTTGYRINSAKDDAAGLQISNRLSNQISGLNVATRNANDGISLA
QTAEGALQQSTNILQRIRDLALQSANGSNSDADRAALQKEVAAQQAELTRISDTTTFGGRKLLDGSFGTTSFQVG
SNAYETIDISLQNASASAIGSYQVGSNGAGTVASVAGTATASGIASGTVNLVGGGQVKNIAIAAGDSAKAIAEKM
DGAIPNLSARARTVFTADVSGVTGGSLNFDVTVGSNTVSLAGVTSTQDLADQLNSNSSKLGITASINDKGVLTIT
SATGENVKFGAQTGTATAGQVAVKVQGSDGKFEAAAKNVVAAGTAATTTIVTGYVQLNSPTAYSVSGTGTQASQV
FGNASAAQKSSVASVDISTADGAQNAIAVVDNALAAIDAQRADLGAVQNRFKNTIDNLTNISENATNARSRIKDT
DFAAETAALSKNQVLQQAGTAILAQANQLPQAVLSLLR*
```

***FliC* consensus sequence of susceptible strains**

```
MALTVNTNIASLNTQRNLNNSSASLNTSLQRLSTGSRINSAKDDAAGLQIANRLTSQVNGLNVATKNANDGISLA
QTAEGALQQSTNILQRMRDLSLQSANGSNSDSERTALNGEVKQLQKELDRISNTTTFGGRKLLDGSFGVASFQVG
--------------------------------------------------------------------------
--------------------------------------------------------------------------
--------------------------------------------------------------------------
-----------------------------------
IDAQRADLGAVQNRFDNTINNLKNIGENVSAARGRIEDTDFAAETANLTKNQVLQQAGTAILAQANQLPQSVLSL
LR*
```

***FliD* consensus sequence of resistant strains**

```
MAGISIGVGSTDYTDLVNKMVNLEGAAKTNQLATLEKTTTTRLTALGQFKSAISAFQTALTALNSNAVFMARTAK
SSNEDILKASATQSAVAGTYQIQVNSLATSSKIALQAIADPANAKFNSGTLNISVGDTKLPAITVDSSNNTLAGM
RDAINQAGKEAGVSATIITDNSGSRLVLSSTKTGDGKDIKVEVSDDGSGGNTSLSQLAFDPATAPKLSDGAAAGY
VTKAANGEITVDGLKRSIASNSVSDVIDGVSFDVKAVTEAGKPITLTVSRDDAGVKDNVKKFVEAYNTLTKFINE
QTVVTKVGEDKNPVTGALLGDASVRALVNTMRSELIASNENGSVRNLAALGITTTKDGTLEIDEKKLDKAISADF
EGVASYFTGDTGLAKRLGDKMKPYTDAQGILDQRTTTLQKTLSNVDTQKADLAKRLAALQEKLTTQFNLLSAMQD
EMTKRQKSITDNLASLPYGSGKKT*
```

***FliD* consensus sequence of susceptible strains**

No blast sequence identified

***FlgK* consensus sequence of resistant strains**

```
MSDLLSIGLSGLGTSQTWLTITGHNITNVKTPGYSRQDAIQQT--
PQFSGAGYMGSGSQIVDVRRLASDFLTGQLRNATSQNSELSAFLGQIDQLNSLLADNTTGVSPAMQRFFSALQTA
AQNPSSTEAREAVLAQAQGLSKTFNTLYDQLDKQNSLINQQLGALTSQVNNLSQSVAEYNDAIAKAKSAGAVPND
LLDARDEAVRKLSEMVGVTAVTQDDNSVSLFIGSGQPLVVGNTVSTLSVVPGLDDPTRYQVQLTLGDSTQNVTRL
VSGGQMGGLLAYRDTVLDSSYNKLGQLALTFADTVNKQLGQGLDLAGKAGANLFGDINDPDITALRVLAKNGNTG
NVHANLNITDTSKLNSSDFRLDFDGTNFTARRLGDDASMQVTVSGTGPYTLSFKDANGVDQGFSVTLDQLPAAGD
RFTLQPTRRGASDIETTLKNASQLAFAGSARAEATTNNRGSGAIGQPNLVGGPSPIDPAVLQNAFGANGLPLSAT
VSADGKTYTMTSPLPAGWSYVDKDGNALPGSPTLNSGTSNSVRMAYTDPGSGQTYTYEFNLSNVPQTGDSFTLSF
NKDGISDNRNALNLNALQTKPTVGGTGSTGSTYNDAYGGLVERVGTLTAQARASADASQTVLKQAQDSRDSLSGV
SLDEEAANLIQFQQYYSASAQVIQVARSLFDTLIGAFR*
```

***FlgK* consensus sequence of susceptible strains**

```
MSDLLSIGLSGLGTSQTWLTITGHNITNVKTPGYSRQDAIQQTQVPQFSGAGYMGSGSQIVDVRRLASDFLTGQL
RNATSQNSELSAFRSQIEQLDGLLSNTTTGVSPAMQRFFAALQAAANNPSSTEAREAVLAQAEGLGKTFNTLYDQ
LDKQNSLINQQLGALASQVNHLSQSVASYNDAIAKAKSAGAVPNDLMDARDEAVRKLSEMIGVTAVTQDDNSVSL
FIGSGQPLVVGNTVSTLSVVPGLDDPTRYQVQLSNGNSIQNVTGLVSGGEMGGLLAYRNSALDSSYNKLGQLAIT
LADTINKQLGQGLDLAGKAGANLFGDINDPDITALRVLAKNGNTGNVHANLNITDTSKLNSSDFRLDFDGTSFTA
RRLGDDASMQVTVSGTGPYTLSFKDANGVDQGFNLTLDQLPAAGDRFTLQPTRRGAADIEATLKNASQLAFAGTA
RTESTTENRGTGKIGAPTLTSGPSPVDPTVLQGAFGPNGISLGATLSADGKTYTLSSPLPAGWSYVDKDGNALTG
SPTLTSGNTNTVRMAFTDP-
SGQKYSYEFELSGVPQNSDSFKLGFNDKGISDNRNALNLLALQTKPTVGGTDNTGSTYNEAYGGLVERVGTLTAQ
VRASSEASATVLKQAQDSRDSLSGVSLDEEAANLIQFQQYYGASAQVIQVARTLFDTLIGAFR*
```

***FlgL* consensus sequence of resistant strains**

MRISTIQAFNNSVSGISRNYADLTRTQAEISAGKRLLTPADDPVGAVRLLQLNQEQALNSQYKSGITAAKNSLQQ
EETILNSVGTVIHRIREIAVQAGNGGLDASDKNALATELAQREDELLNLLNSRDASGKYLFSGSQGDTQPFVRNP
DGTYSYNGDEGQREVQIASSTFIAISDNGKILFESGSNANRVSTGKDAAGLDASGNPSDSSISLGLVTDKEAYDT
VFPSSTPPLASDGVGIHFTDAKNYVVYDLKTIPPGYDWSTSDPNPP-
SFATLASGKIDDNAQTSDFITFGGVKVQIDGEPQGGDTFSIKRQPDQEKRSLLNTVSDLRKALLSAEDTPAGNLA
IRDAVGVAISNLDSSNSQILTGQGRIGARMNVAESTETFIDDVTLVNTAVISQIQDLDYPEALSRLTLQSTIMDA
AQQSFVKIRGLSLFNYLS*

***FlgL* consensus sequence of susceptible strains**

MRISTIQAFNNSVNGISRNYADLNRTFEQISTGKRILTPADDPVGSVRLLRLDQEQGLNEQYKTGMTEAKNSLSQ
EETILRSVGNVLQRIREIAGQAGDGALDSNDKKSLASELRQREDELLNLLNSRDASGKYLFSGSQGSVQPFVRNE
DGTYSYMGDESQREVQIASSTRIPVSDSGKVLFEDIVNAARLDT-------
AAAGNTGDGRISVGLVEDELAFDSQFPASNPPAATDGFNIHFVSDKEYVVYDPKSLPPGYDWTTYDPNSPPAWQ-
LSKGAIDDDPKTIDKVLYAGVSVTIDGTPKAGDEFNVNYKPGSEKRSLLNVVSDLRKALESSTDNQAGNDAIRDA
TAVALTNLSAVAAAVDGGQGKIGARLNTVESTETFIDDVKLVNASVMSQIQDLDYAEALSRLSLQSTIMDAAQQS
YVKIQGLSLFNYL--

a

gene	gene name
1	cytochrome c oxidase
2	hypothetical protein
3	alpha-1,6-rhamnosyltransferase **MigA**
4	conserved hypothetical protein
5	conserved hypothetical protein
6	secreted protein Hcp
7	hypothetical protein
8	excinuclease ABC subunit C
9	hypothetical protein
10	NADH dehydrogenase I chain C
11	geranyl-CoA carboxylase
12	B-band O-antigen polymerase **wzy**
13	probable oxidoreductase
14	conserved hypothetical protein
15	DNA mismatch repair protein MutS
16	respiratory nitrate reductase beta chain
17	probable acyl-CoA dehydrogenase
18	soluble and membrane-bound lytic transglycosylases
19	glucose-6-phosphate isomerase
20	conserved hypothetical protein
21	DNA mismatch repair protein MutL
22	probable two-component response regulator
23	cell surface-sugar biosynthetic glycosyltransferase **ssg**
24	**WapH**
25	glycine-cleavage system protein T1
26	hypothetical protein
27	hypothetical protein
28	MifR
29	Uncharacterized protein

b

gene	gene name
1	tryptophan synthase beta chain
2	cytochrome c oxidase
3	malonate transporter MadM
4	probable CoA transferase
5	hypothetical protein
6	hypothetical protein
7	alpha-1,6-rhamnosyltransferase **MigA**
8	probable heat shock protein (hsp90 family)
9	secreted protein Hcp
10	sigma factor regulator
11	hypothetical protein
12	conserved hypothetical protein
13	putative lipase
14	probable secretion protein
15	DNA mismatch repair protein MutS
16	MexJ
17	Resistance-Nodulation-Cell Division (RND) multidrug efflux transporter MexW
18	hypothetical protein
19	probable acyl-CoA dehydrogenase
20	hypothetical protein
21	glucose-6-phosphate isomerase
22	DNA mismatch repair protein MutL
23	probable two-component response regulator
24	cell surface-sugar biosynthetic glycosyltransferase **ssg**
25	**WapH**
26	conserved hypothetical protein
27	conserved hypothetical protein
28	HocS
29	hypothetical protein
30	Uncharacterized protein

Supplementary Figure 5: Full legend to the volcano plots for LPS-5 at MOI 0.1 (a.) and MOI20 (b.).

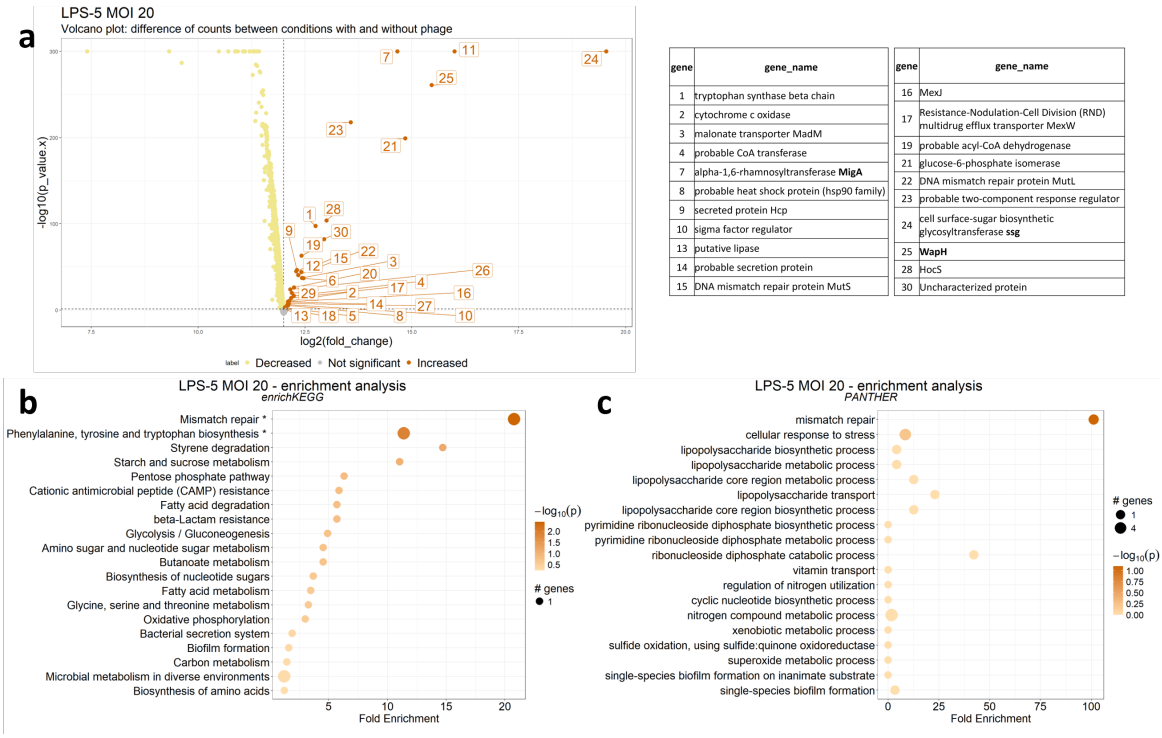

gene	gene_name
1	tryptophan synthase beta chain
2	cytochrome c oxidase
3	malonate transporter MadM
4	probable CoA transferase
7	alpha-1,6-rhamnosyltransferase **MigA**
8	probable heat shock protein (hsp90 family)
9	secreted protein Hcp
10	sigma factor regulator
13	putative lipase
14	probable secretion protein
15	DNA mismatch repair protein MutS

gene	gene_name
16	MexJ
17	Resistance-Nodulation-Cell Division (RND) multidrug efflux transporter MexW
19	probable acyl-CoA dehydrogenase
21	glucose-6-phosphate isomerase
22	DNA mismatch repair protein MutL
23	probable two-component response regulator
24	cell surface-sugar biosynthetic glycosyltransferase **ssg**
25	**WapH**
28	HocS
30	Uncharacterized protein

Supplementary Figure 6: **a,** This volcano plot describes genes with a significant difference in counts (fold change) between conditions with and without LPS-5 phage at MOI 0.1. Like the previous plot, orange signifies a significant increase in gene counts, yellow stands for a significant decrease, and gray represents non-significant genes. **b,** Similar to the previous functional analysis plot, this section summarizes the functional enrichment analysis results for the LPS-5 phage at MOI 0.1 with enrichKEGG. **c,** Key functional categories identified through the more detailed PANTHER analysis are linked to LPS and LPS biosynthesis, providing insights into the enriched functions specific to the LPS-5 phage.

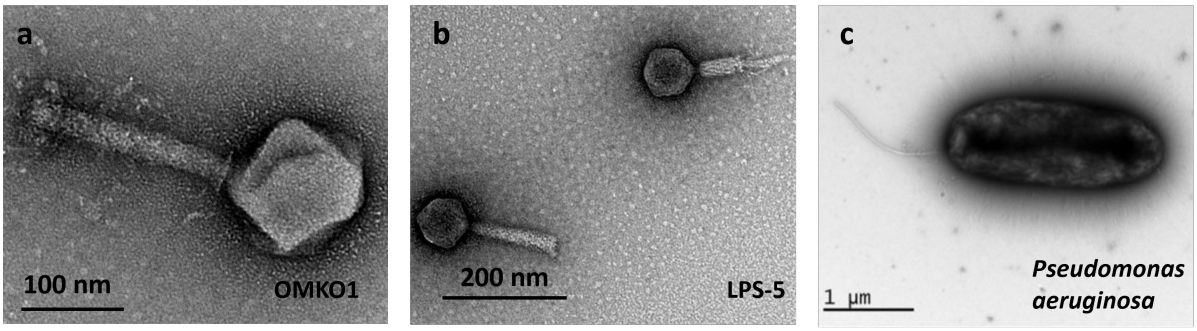

d

Phage	OMKO1	LPS-5
Plaque characteristics	Clear, well-circumscribed Size: 0.5-1.5mm	Clear, well-circumscribed Size: 1.5-2.0mm
genome	278kb	unknown
Tail length	212 ± 2nm	140 ± 2nm
Tail width	28 ± 1nm	20 ± 1nm
Head length	134 ± 4nm	70 ± 3nm
Head shape	Isomeric	Isomeric
Family	Myoviridae	Myoviridae

Supplementary Figure 7: **Bacteriophages OMKO1, LPS-5 and their host Pseudomonas Aeruginosa. a,** Transmission electron microscopy (TEM) image of phage OMKO1. **b,** TEM image of LPS-5 phage. **c,** TEM image of Pseudomonas Aeruginosa, the natural host of phages OMKO1 and LPS-5. **d,** Characteristics of phages OMKO1 and LPS-5.

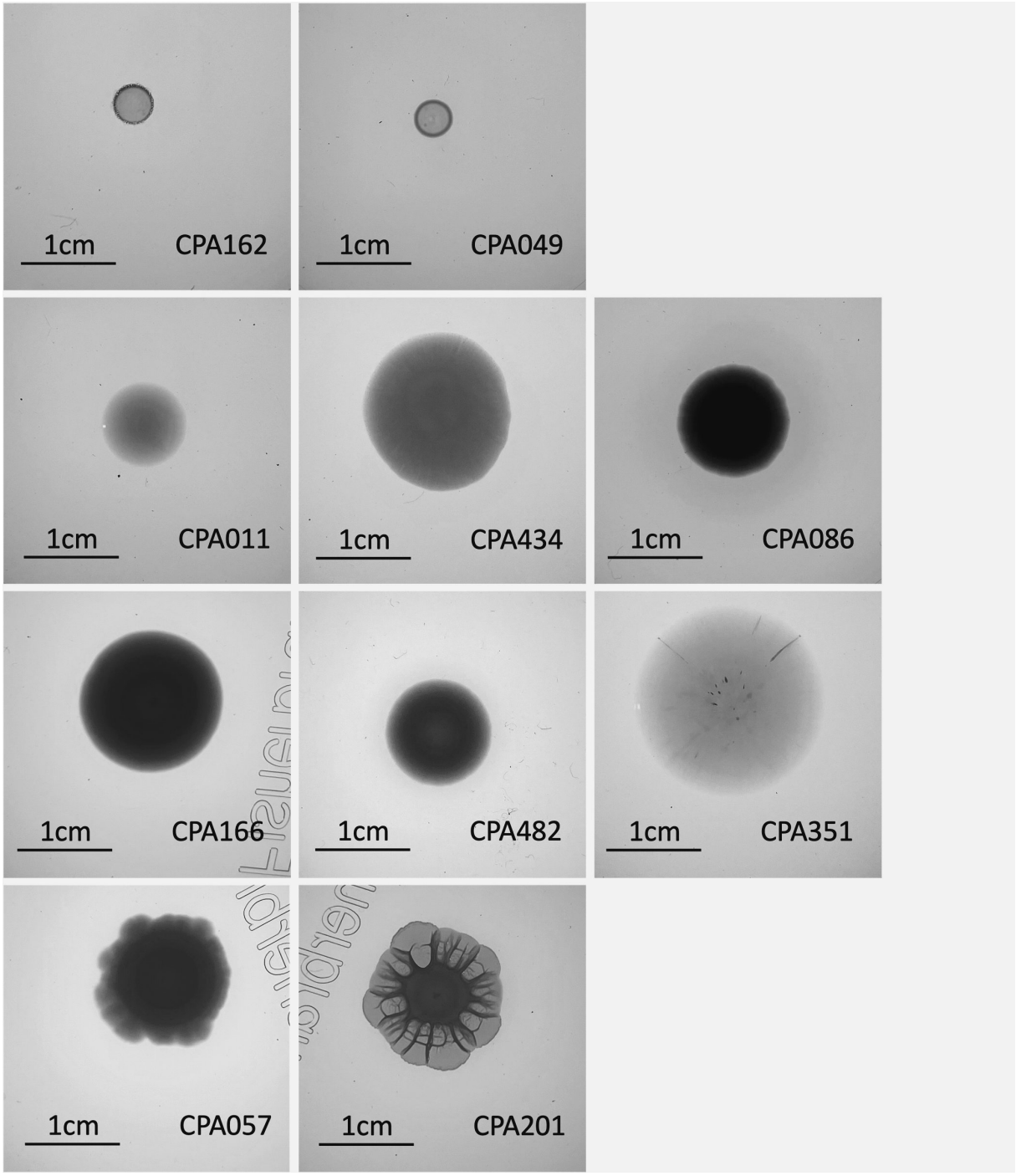
1cm
CPA162
1cm
CPA049
1cm
CPA011
1cm
CPA434
1cm
CPA086
1cm
CPA166
1cm
CPA482
1cm
CPA351
1cm
CPA057
1cm
CPA201

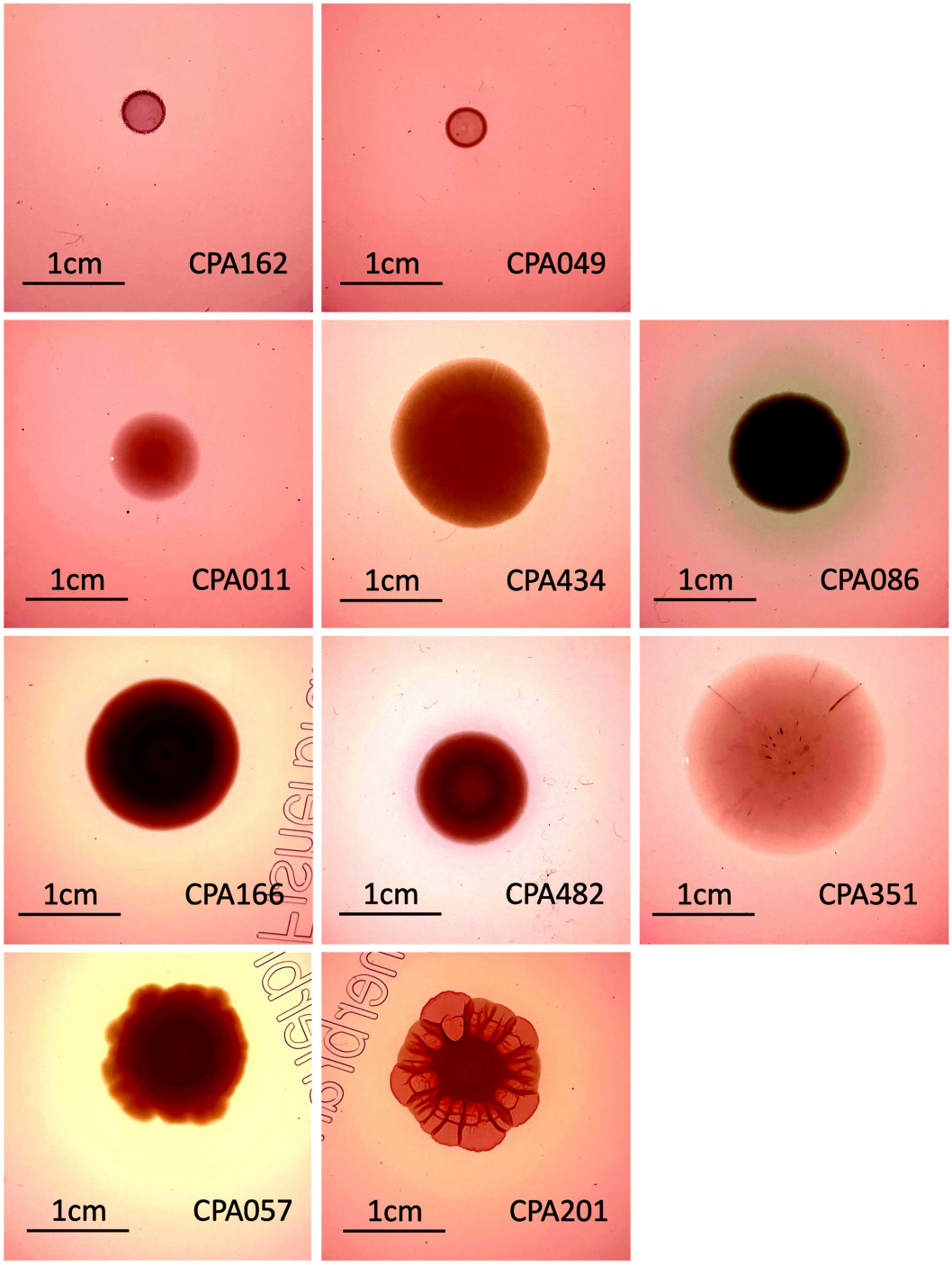

Supplementary Figure 8: O-AG/LPS morphology of the clinical isolates.

Flagella gene	**RefSeq**
fliD	NP_249785.1
fliC	NP_249783.1
flgL	NP_249778.1
flgK	NP_249777.1
flgE	NP_249771.1
flgG	NP_249773.1
flgH	NP_249774.1
flgI	NP_249775.1
flgB	NP_249768.1
flgC	NP_249769.1
flgF	NP_249772.1
fliE	NP_249791.1
fliO	NP_250136.1
fliP	NP_250137.1
fliQ	NP_250138.1
fliR	NP_250139.1
fliF	NP_249792.1
fliG	NP_249793.1
fliY	NP_249005.1
fliM	NP_250134.1
fliN	NP_250135.1
flhA	NP_250143.1
flhB	NP_250140.1
fliH	NP_249794.1
fliI	NP_249795.1
fliJ	NP_249796.1
LPS biosynthetic gene	**RefSeq**
migA	NP_249396.1
wzy	NP_251844.1
wapH	NP_253691.1
ssg	NP_253688.1

Supplementary Figure 9: Flagella and LPS biosynthetic reference sequences from Pseudomonas genome database.[72]

References

1. Murray CJL, Ikuta KS, Sharara F, et al. Global burden of bacterial antimicrobial resistance in 2019: a systematic analysis. *The Lancet*. 2022;399(10325):629-655. doi:10.1016/S0140-6736(21)02724-0
2. Pachori P, Gothalwal R, Gandhi P. Emergence of antibiotic resistance Pseudomonas aeruginosa in intensive care unit; a critical review. *Genes Dis*. 2019;6(2):109-119. doi:10.1016/j.gendis.2019.04.001
3. Jorth P, Staudinger BJ, Wu X, et al. Regional Isolation Drives Bacterial Diversification within Cystic Fibrosis Lungs. *Cell Host Microbe*. 2015;18(3):307-319. doi:10.1016/j.chom.2015.07.006
4. Wood SJ, Kuzel TM, Shafikhani SH. Pseudomonas aeruginosa: Infections, Animal Modeling, and Therapeutics. *Cells*. 2023;12(1):199. doi:10.3390/cells12010199
5. Oromí-Bosch A, Antani JD, Turner PE. Developing Phage Therapy That Overcomes the Evolution of Bacterial Resistance. *Annu Rev Virol*. 2023;10(1):503-524. doi:10.1146/annurev-virology-012423-110530
6. Du Toit A. The language of phages. *Nat Rev Microbiol*. 2017;15(3):135-135. doi:10.1038/nrmicro.2017.8
7. Hulo C, de Castro E, Masson P, et al. ViralZone: a knowledge resource to understand virus diversity. *Nucleic Acids Res*. 2011;39(Database issue):D576-582. doi:10.1093/nar/gkq901
8. Labrie SJ, Samson JE, Moineau S. Bacteriophage resistance mechanisms. *Nat Rev Microbiol*. 2010;8(5):317-327. doi:10.1038/nrmicro2315
9. Hampton HG, Watson BNJ, Fineran PC. The arms race between bacteria and their phage foes. *Nature*. 2020;577(7790):327-336. doi:10.1038/s41586-019-1894-8
10. Ackermann HW. Who went into phage research? *Bacteriophage*. 2012;2(1):55-59. doi:10.4161/bact.18680
11. McCallin, Sacher, Zheng, Chan. Current State of Compassionate Phage Therapy. *Viruses*. 2019;11(4):343. doi:10.3390/v11040343
12. Aslam S, Lampley E, Wooten D, et al. Lessons Learned From the First 10 Consecutive Cases of Intravenous Bacteriophage Therapy to Treat Multidrug-Resistant Bacterial Infections at a Single Center in the United States. *Open Forum Infect Dis*. 2020;7(9):ofaa389. doi:10.1093/ofid/ofaa389
13. Wright A, Hawkins CH, Änggård EE, Harper DR. A controlled clinical trial of a therapeutic bacteriophage preparation in chronic otitis due to antibiotic-resistant *Pseudomonas aeruginosa* ; a preliminary report of efficacy. *Clin Otolaryngol*. 2009;34(4):349-357. doi:10.1111/j.1749-4486.2009.01973.x
14. Terwilliger AL, Gu Liu C, Green SI, et al. Tailored Antibacterials and Innovative Laboratories for Phage (Φ) Research: Personalized Infectious Disease Medicine for the Most Vulnerable At-Risk Patients. *PHAGE*. 2020;1(2):66-74. doi:10.1089/phage.2020.0007
15. Khatami A, Foley DA, Warner MS, et al. Standardised treatment and monitoring protocol to assess safety and tolerability of bacteriophage therapy for adult and paediatric patients (STAMP study): protocol for an open-label, single-arm trial. *BMJ Open*. 2022;12(12):e065401. doi:10.1136/bmjopen-2022-065401
16. Chan BK, Turner PE, Kim S, Mojibian HR, Elefteriades JA, Narayan D. Phage treatment of an aortic graft infected with *Pseudomonas aeruginosa*. *Evol Med Public Health*. 2018;2018(1):60-66. doi:10.1093/emph/eoy005
17. Sarker SA, Sultana S, Reuteler G, et al. Oral Phage Therapy of Acute Bacterial Diarrhea With Two Coliphage Preparations: A Randomized Trial in Children From Bangladesh. *EBioMedicine*. 2016;4:124-137. doi:10.1016/j.ebiom.2015.12.023
18. Jault P, Leclerc T, Jennes S, et al. Efficacy and tolerability of a cocktail of bacteriophages to treat burn wounds infected by Pseudomonas aeruginosa (PhagoBurn): a randomised, controlled, double-blind phase 1/2 trial. *Lancet Infect Dis*. 2019;19(1):35-45. doi:10.1016/S1473-3099(18)30482-1
19. Jia HJ, Jia PP, Yin S, Bu LK, Yang G, Pei DS. Engineering bacteriophages for enhanced host range and efficacy: insights from bacteriophage-bacteria interactions. *Front Microbiol*. 2023;14:1172635. doi:10.3389/fmicb.2023.1172635
20. Ando H, Lemire S, Pires DP, Lu TK. Engineering Modular Viral Scaffolds for Targeted Bacterial Population Editing. *Cell Syst*. 2015;1(3):187-196. doi:10.1016/j.cels.2015.08.013
21. Pourcel C, Midoux C, Vergnaud G, Latino L. The Basis for Natural Multiresistance to Phage

in Pseudomonas aeruginosa. *Antibiotics*. 2020;9(6):339. doi:10.3390/antibiotics9060339
22. Bickle TA. Restricting restriction. *Mol Microbiol*. 2004;51(1):3-5. doi:10.1046/j.1365-2958.2003.03846.x
23. Vasu K, Nagaraja V. Diverse Functions of Restriction-Modification Systems in Addition to Cellular Defense. *Microbiol Mol Biol Rev*. 2013;77(1):53-72. doi:10.1128/MMBR.00044-12
24. Barrangou R, Fremaux C, Deveau H, et al. CRISPR Provides Acquired Resistance Against Viruses in Prokaryotes. *Science*. 2007;315(5819):1709-1712. doi:10.1126/science.1138140
25. Mohanraju P, Makarova KS, Zetsche B, Zhang F, Koonin EV, Van Der Oost J. Diverse evolutionary roots and mechanistic variations of the CRISPR-Cas systems. *Science*. 2016;353(6299):aad5147. doi:10.1126/science.aad5147
26. Chan BK, Sistrom M, Wertz JE, Kortright KE, Narayan D, Turner PE. Phage selection restores antibiotic sensitivity in MDR Pseudomonas aeruginosa. *Sci Rep*. 2016;6(1):26717. doi:10.1038/srep26717
27. Chan B, Stanley G, Kortright K, et al. *Personalized Inhaled Bacteriophage Therapy Decreases Multidrug-Resistant* Pseudomonas Aeruginosa. Respiratory Medicine; 2023. doi:10.1101/2023.01.23.22283996
28. Smith EE, Buckley DG, Wu Z, et al. Genetic adaptation by *Pseudomonas aeruginosa* to the airways of cystic fibrosis patients. *Proc Natl Acad Sci*. 2006;103(22):8487-8492. doi:10.1073/pnas.0602138103
29. Kim MK, Chen Q, Echterhof A, et al. A Blueprint for Broadly Effective Bacteriophage Therapy Against Bacterial Infections. Published online April 21, 2024. doi:10.1101/2024.04.20.590411
30. Han P, Lin W, Fan H, Tong Y. Characterization of phage evolution and phage resistance in drug-resistant *Stenotrophomonas maltophilia*. Lowen AC, ed. *J Virol*. 2024;98(2):e01249-23. doi:10.1128/jvi.01249-23
31. Koderi Valappil S, Shetty P, Deim Z, et al. Survival Comes at a Cost: A Coevolution of Phage and Its Host Leads to Phage Resistance and Antibiotic Sensitivity of Pseudomonas aeruginosa Multidrug Resistant Strains. *Front Microbiol*. 2021;12:783722. doi:10.3389/fmicb.2021.783722
32. Nobrega FL, Vlot M, De Jonge PA, et al. Targeting mechanisms of tailed bacteriophages. *Nat Rev Microbiol*. 2018;16(12):760-773. doi:10.1038/s41579-018-0070-8
33. Guerrero-Ferreira RC, Viollier PH, Ely B, et al. Alternative mechanism for bacteriophage adsorption to the motile bacterium *Caulobacter crescentus*. *Proc Natl Acad Sci*. 2011;108(24):9963-9968. doi:10.1073/pnas.1012388108
34. Choi Y, Shin H, Lee JH, Ryu S. Identification and Characterization of a Novel Flagellum-Dependent Salmonella-Infecting Bacteriophage, iEPS5. *Appl Environ Microbiol*. 2013;79(16):4829-4837. doi:10.1128/AEM.00706-13
35. Raimondo LM, Lundh NP, Martinez RJ. Primary Adsorption Site of Phage PBS1: the Flagellum of *Bacillus subtilis*. *J Virol*. 1968;2(3):256-264. doi:10.1128/jvi.2.3.256-264.1968
36. Lovett PS. PBP1: A flagella specific bacteriophage mediating transduction in Bacillus pumilus. *Virology*. 1972;47(3):743-752. doi:10.1016/0042-6822(72)90564-8
37. Esteves NC, Scharf BE. Flagellotropic Bacteriophages: Opportunities and Challenges for Antimicrobial Applications. *Int J Mol Sci*. 2022;23(13):7084. doi:10.3390/ijms23137084
38. Gurney J, Pradier L, Griffin JS, et al. Phage steering of antibiotic-resistance evolution in the bacterial pathogen, Pseudomonas aeruginosa. *Evol Med Public Health*. 2020;2020(1):148-157. doi:10.1093/emph/eoaa026
39. Gambino M, Sørensen MCH. Flagellotropic phages: common yet diverse host interaction strategies. *Curr Opin Microbiol*. 2024;78:102451. doi:10.1016/j.mib.2024.102451
40. Li Y, Guan J, Hareendranath S, et al. A family of novel immune systems targets early infection of nucleus-forming jumbo phages. Published online September 18, 2022. doi:10.1101/2022.09.17.508391
41. Harvey H, Bondy-Denomy J, Marquis H, Sztanko KM, Davidson AR, Burrows LL. Pseudomonas aeruginosa defends against phages through type IV pilus glycosylation. *Nat Microbiol*. 2017;3(1):47-52. doi:10.1038/s41564-017-0061-y
42. Huszczynski SM, Lam JS, Khursigara CM. The Role of Pseudomonas aeruginosa Lipopolysaccharide in Bacterial Pathogenesis and Physiology. *Pathog Basel Switz*. 2019;9(1):6. doi:10.3390/pathogens9010006

43. Kortright KE, Chan BK, Evans BR, Turner PE. Arms race and fluctuating selection dynamics in *Pseudomonas aeruginosa* bacteria coevolving with phage OMKO1. *J Evol Biol*. 2022;35(11):1475-1487. doi:10.1111/jeb.14095
44. Mukherjee S, Moustafa DA, Stergioula V, Smith CD, Goldberg JB, Bassler BL. The PqsE and RhlR proteins are an autoinducer synthase–receptor pair that control virulence and biofilm development in *Pseudomonas aeruginosa*. *Proc Natl Acad Sci*. 2018;115(40). doi:10.1073/pnas.1814023115
45. Markwitz P, Lood C, Olszak T, Van Noort V, Lavigne R, Drulis-Kawa Z. Genome-driven elucidation of phage-host interplay and impact of phage resistance evolution on bacterial fitness. *ISME J*. 2022;16(2):533-542. doi:10.1038/s41396-021-01096-5
46. De Smet J, Zimmermann M, Kogadeeva M, et al. High coverage metabolomics analysis reveals phage-specific alterations to *Pseudomonas aeruginosa* physiology during infection. *ISME J*. 2016;10(8):1823-1835. doi:10.1038/ismej.2016.3
47. Olszak T, Augustyniak D, García-Romero I, et al. Phage treatment of Pseudomonas aeruginosa yields a phage-resistant population with different susceptibility to innate immune responses and mild effects on metabolic profiles. *Microbiol Res*. 2024;282:127609. doi:10.1016/j.micres.2024.127609
48. Pitcher RS, Tonkin LM, Daley JM, et al. Mycobacteriophage Exploit NHEJ to Facilitate Genome Circularization. *Mol Cell*. 2006;23(5):743-748. doi:10.1016/j.molcel.2006.07.009
49. Dupuis MÈ, Villion M, Magadán AH, Moineau S. CRISPR-Cas and restriction–modification systems are compatible and increase phage resistance. *Nat Commun*. 2013;4(1):2087. doi:10.1038/ncomms3087
50. Seed KD. Battling Phages: How Bacteria Defend against Viral Attack. Miller VL, ed. *PLOS Pathog*. 2015;11(6):e1004847. doi:10.1371/journal.ppat.1004847
51. Deveau H, Garneau JE, Moineau S. CRISPR/Cas System and Its Role in Phage-Bacteria Interactions. *Annu Rev Microbiol*. 2010;64(1):475-493. doi:10.1146/annurev.micro.112408.134123
52. Costa AR, Van Den Berg DF, Esser JQ, et al. Accumulation of defense systems in phage-resistant strains of *Pseudomonas aeruginosa*. *Sci Adv*. 2024;10(8):eadj0341. doi:10.1126/sciadv.adj0341
53. Essoh C, Blouin Y, Loukou G, et al. The Susceptibility of Pseudomonas aeruginosa Strains from Cystic Fibrosis Patients to Bacteriophages. Kaufmann GF, ed. *PLoS ONE*. 2013;8(4):e60575. doi:10.1371/journal.pone.0060575
54. Mutalik VK, Adler BA, Rishi HS, et al. High-throughput mapping of the phage resistance landscape in E. coli. De Visser JAGM, ed. *PLOS Biol*. 2020;18(10):e3000877. doi:10.1371/journal.pbio.3000877
55. Patel PH, Maxwell KL. Prophages provide a rich source of antiphage defense systems. *Curr Opin Microbiol*. 2023;73:102321. doi:10.1016/j.mib.2023.102321
56. Rollie C, Chevallereau A, Watson BNJ, et al. Targeting of temperate phages drives loss of type I CRISPR–Cas systems. *Nature*. 2020;578(7793):149-153. doi:10.1038/s41586-020-1936-2
57. Mutalik VK, Novichkov PS, Price MN, et al. Dual-barcoded shotgun expression library sequencing for high-throughput characterization of functional traits in bacteria. *Nat Commun*. 2019;10(1):308. doi:10.1038/s41467-018-08177-8
58. Payne LJ, Todeschini TC, Wu Y, et al. Identification and classification of antiviral defence systems in bacteria and archaea with PADLOC reveals new system types. *Nucleic Acids Res*. 2021;49(19):10868-10878. doi:10.1093/nar/gkab883
59. Bernheim A, Sorek R. The pan-immune system of bacteria: antiviral defence as a community resource. *Nat Rev Microbiol*. 2020;18(2):113-119. doi:10.1038/s41579-019-0278-2
60. Jacobs MA, Alwood A, Thaipisuttikul I, et al. Comprehensive transposon mutant library of *Pseudomonas aeruginosa*. *Proc Natl Acad Sci*. 2003;100(24):14339-14344. doi:10.1073/pnas.2036282100
61. Fisher RA. The Logic of Inductive Inference. *J R Stat Soc*. 1935;98(1):39. doi:10.2307/2342435
62. Yu G, Wang LG, Han Y, He QY. clusterProfiler: an R Package for Comparing Biological Themes Among Gene Clusters. *OMICS J Integr Biol*. 2012;16(5):284-287. doi:10.1089/omi.2011.0118
63. Mi H, Ebert D, Muruganujan A, et al. PANTHER version 16: a revised family classification,

tree-based classification tool, enhancer regions and extensive API. *Nucleic Acids Res*. 2021;49(D1):D394-D403. doi:10.1093/nar/gkaa1106
64. Jaillard M, Lima L, Tournoud M, et al. A fast and agnostic method for bacterial genome-wide association studies: Bridging the gap between k-mers and genetic events. Didelot X, ed. *PLOS Genet*. 2018;14(11):e1007758. doi:10.1371/journal.pgen.1007758
65. ncbi. BLAST® Command Line Applications User Manual. Published online June 23, 2008. https://www.ncbi.nlm.nih.gov/books/NBK279670/
66. Katoh K. MAFFT: a novel method for rapid multiple sequence alignment based on fast Fourier transform. *Nucleic Acids Res*. 2002;30(14):3059-3066. doi:10.1093/nar/gkf436
67. Rice P, Longden I, Bleasby A. EMBOSS: The European Molecular Biology Open Software Suite. *Trends Genet*. 2000;16(6):276-277. doi:10.1016/S0168-9525(00)02024-2
68. Hornik K. Wilcoxon test. https://web.mit.edu/~r/current/arch/i386_linux26/lib/R/library/stats/html/Wilcoxon.html
69. Davies S, Ihaka R. glm. https://stat.ethz.ch/R-manual/R-devel/library/stats/html/glm.html
70. Perkel JM. The software that powers scientific illustration. *Nature*. 2020;582(7810):137-138. doi:10.1038/d41586-020-01404-7
71. Siryaporn A, Kim MK, Shen Y, Stone HA, Gitai Z. Colonization, Competition, and Dispersal of Pathogens in Fluid Flow Networks. *Curr Biol*. 2015;25(9):1201-1207. doi:10.1016/j.cub.2015.02.074
72. Winsor GL, Griffiths EJ, Lo R, Dhillon BK, Shay JA, Brinkman FSL. Enhanced annotations and features for comparing thousands of Pseudomonas genomes in the Pseudomonas genome database. *Nucleic Acids Res*. 2016;44(D1):D646-653. doi:10.1093/nar/gkv1227
73. Bolger AM, Lohse M, Usadel B. Trimmomatic: a flexible trimmer for Illumina sequence data. *Bioinformatics*. 2014;30(15):2114-2120. doi:10.1093/bioinformatics/btu170
74. Prjibelski A, Antipov D, Meleshko D, Lapidus A, Korobeynikov A. Using SPAdes De Novo Assembler. *Curr Protoc Bioinforma*. 2020;70(1):e102. doi:10.1002/cpbi.102
75. Conover WJ. On Methods of Handling Ties in the Wilcoxon Signed-Rank Test. *J Am Stat Assoc*. 1973;68(344):985-988. doi:10.1080/01621459.1973.10481460
76. Portet S. A primer on model selection using the Akaike Information Criterion. *Infect Dis Model*. 2020;5:111-128. doi:10.1016/j.idm.2019.12.010
77. Hartig F. DHARMa. Published online September 8, 2022. https://cran.r-project.org/web/packages/DHARMa/vignettes/DHARMa.html